Deanship of Graduate Studies
Al – Quds University

DNA Condensation Using Cationic Dendrimer

Marwa Ibrahim Mohammad Abuzer

M.Sc. Thesis

Jerusalem – Palestine

1437 / 2016

DNA Condensation Using Cationic Dendrimer

Prepared By

Marwa Ibrahim Mohammad Abuzer

B. Sc., Physics, Al-Quds University -Palestine

Supervisor
Dr. Khawla Qamhieh

A thesis submitted artial fulfillment of the requirements for the degree of Master of in Physics

Jerusalem – Palestine
2016 / 1437

Al – Quds University
Deanship of Graduate Studies

Physics Department

Thesis Approval

DNA Condensation Using Cationic Dendrimer

Marwa Ibrahim Abuzer.
Registration No: 21110787

Supervisor:

Dr. Khawla Qamhieh

Master thesis submitted and accepted, 3 /1 / 2016 The name and signature of examining committee members are as follows

1. Head of the committee: Dr. Khawla Qamhieh Signature: .....
2. Internal Examiner: Prof .Dr. Imad A. Barghouthi Signature: .....
3. External Examiner: Dr. Jamal Afif Ghabboun Signature: .....

Jerusalem – Palestine

1437 / 2016

Dedication

I dedicate this thesis to all of my wonderful family members who have supported me throughout my life and allowed me to achieve my goals

To my father Ibrahim, who helped in making my educational decisions and sent me on the path to my graduate career; to my mother Nadia, who raised me to be the person I am today. She has been with me on every step of the way, through good and bad times. Thank you for all the unconditional love, guidance, and support that you have always given me, and for helping me to succeed and instilling in me the confidence that I am capable of doing anything I put my mind to. To my husband , Ahmad , for his encouragement and support; to my supporting brother, my nice sister and my son Mahmoud who gave me more reasons to succeed; and to any future child… I just don't know who you are yet. Thank you for
everything. I love you!

Declaration

*I here*by declare that this thesis is based on the results found by myself. Materials of works found by other researchers are mentioned by references. This thesis, neither in whole or in part, has been previously submitted for any degree

The work was done under the supervision of Dr. Khawla Qamhieh, at Al – Quds University, Palestine

Marwa Ibrahim Abuzer

Acknowledgements

At first and at last, my great commendation and thanks go to Allah, who gave me the ability to accomplish this work, and create such nice supporting people

I would like to thank all those people who deserve my gratitude and made this thesis possible and an enjoyable experience for me

First of all, I wish to express my sincere gratitude to my supervisor Dr. Khawla Qamhieh not only for the support she gave me during my research, but most of all for providing the ability to work in stimulating environment eager of discovery and continuous learning

Acknowledgements are due to AL- Quds University

Special thanks go to my husband who has unwavering encouragement, kindness, incorporeal support to me and has supported me in achieving my dream of obtaining a master degree. Where would I be without my family? My parents deserve special mentioning for their inseparable support and prayers. My father, in the first place , is the person who put the fundament in my learning character, showing me the joy of intellectual pursuit ever since I was a child. My mother is the one who sincerely raised me with her caring and gently love. Thank you

Abstract

The complex build–up of biomaterials consist of biopolymers, namely DNA, and the soft particles poly amidoamine (PAMAM) dendrimers of generation G1, G2, G3, G4, G6 and G8 have been studied by using a new developed theoretical model by Qamhieh and co-workers who described the interaction between linear polyelectrolyte (LPE) chain and ion-penetrable sphere. Many factors are investigated such as the dendrimer size generation, the Bjerrum length, salt concentration, and rigidity of the LPE chain (Persistence length) that affect the dendrimer/LPE complex.

Through the complexation of LPE chain with one dendrimer, it has been found that the wrapping degree of the chain around dendrimer increases by increasing the dendrimer`s generation, the Bjerrum length,and the salt concentration and it decreases by increasing the Persistence length. It has been found that the optimal wrapping length of the LPE chain around dendrimer depends only on the dendrimer generation. In addition the effect of 1:1 salt concentration on complexation of DNA plasmids with one dendrimer of different generation has been studied.

Complexes formed between multiple PAMAM dendrimers and oppositely charged LPE chain depends on the generation of dendrimer. It has been shown that the optimal wrapping length increases while the linker between dendrimers decreases .This result is in agreement with the previous result of Qamhieh and co-workers studies for other generations of dendrimers.

Table of Contents

Table of Contents

List of Tables

List of Figures

List of Abbreviations:

Symbol	Abbreviation representation
DNA	Deoxyribonucleic acid
LPE	Linear Polyelectrolyte
PAMAM	Poly(amido amine)
N_{ch}	Number of the monomers on the chain
Z_{dend}	Number of functional groups of dendrimer
TEM	Transmission electron microscopy
MD	Molecular Dynamic
BD	Brownian Dynamic
CG	Coarse – grained
bp	base – pair
l_{opt}	The optimal wrapping length of chain around dendrimer
l_{iso}	The length of the chain needed to neutralize the charge of dendrimer
DLS	Dynamic Light Scattering
l_p	The persistence length of LPE chain
PEG	Poly(Ethylene Glycol)
N_{exp}	The number of dendrimer bound per DNA moleculer

Chapter ONE

INTRODUCTION

Chapter One: Introduction

1. Introduction

Gene therapy is the insertion of genes into an individual's cells and tissues to treat a disease, such as a hereditary disease in which a deleterious mutant allele is replaced with a functional one.

DNA diameter is about 2 nm, while the length of a stretched single DNA molecule may be up to several meters, and it should take place in the nuclei of the cell with few nms. The challenge is how to compact the DNA in this size to deliver it in the cell. This process – compacting DNA- is called DNA condensation, using one or more of dendrimers - highly branched, star-shaped macromolecules with nanometer-scale dimensions.where the DNA is wrapping around the dendrimers. Non-viral vectors like dendrimer are attractive because of their lower immunogenicity, greater safety and ease of preparation **[Kataoka and Harashima, 2001] [Itaka and Kataoka, 2009]**. In addition, chemical vectors can be formulated via a simple routine pharmaceutical process, and are increasingly used in experiments in vitro, and in clinical trials **[Nomani et al. 2010]**. The dendrimers provide the polyelectrolyte with an effective protection from the influence of surrounding medium **[Lyulin et.al, 2008].**

DNA collapse, or condensation, can occur spontaneously in the test tube, upon adding a low concentration of multivalent action to low ionic strength aqueous buffer **[Gosule and Schellman, 1976]**.In addition condensation is affected by salt concentration **[Netz and Jonny, 1999]**. The charges of the complexation is affected by the solvent quality **[Dobrynin, 2001]**, radius of macroion **[Chodanowski, 2001]**, and flexibility of LPE **[Akinchina, 2002]**. Nguyen and Shklovskii had showed that the complex formation is affected by the charge ratio of the DNA concentrations. The electrostatic repulsive force leads to increase the dendrimer radius **[Dootz, 2008]**.The manning counterion condensation theory states that 90% of the DNA charges need to be neutralized for the DNA condensation **[manning, 1978]**. Most of the complexes Dendrimer/DNA with organized internal structure have been found to self-organize into two-dimensional hexagonal or

square lattices depending on factors such as dendrimer generation and degree of protonation **[Ainalem, 2011]**.

The wrapping degree of the chain around the dendrimer increases by increasing dendrimers charge (decreasing pH), Bjerum length, salt concentration, and decreases by increasing the rigidity of the chain **[Qamhieh, 2013]**.Effects of ionic strength on the diameter of toroidal condensates, originates from the increasing correlation distance between condensed counterions **[Liu, 2012]**.

Dendrimers can mimic biological macromolecules such as enzymes, viral protein, antibodies, histones, and polyamine such as spermine and spermidine **[Tomalia et al., 1990]**, **[Bielinska et al., 1999**], As a consequence dendrimers form stable complexes with DNA and protect DNA against degradation **[Wang et at., 2010], [Fant et al., 2010].** Such properties make dendrimer excellent tools for gene delivery **[Lee et al., 2005]**. Charge of DNA/dendrimer complex is negative for all dendrimers when $r_{charge} < 1$, **[Qamhieh, 2009]**.The number of DNA turns around a dendrimer depends on the size or generation of the dendrimer [**Qamhieh, 2009]**. The process of DNA condensation strongly depends on the speed of adding multivalent cations, and more steps of adding cation ,the more compact the condensed DNA structure will be **[Chai, 2013]**.

Lyulin studied the complex formation between one LPE chain and two dendrimers and found that the dendrimers are sufficiently overcharged, and the degree of overcharging increases with the increase of the LPE length and is accompanied by the linker between dendrimers- which is a part of nonadsorped monomers of LPE- until saturation in overcharging is reached **[Lyulin et al.,2010]**.

The challenge for biophysicists is to establish the relationship between a certain Nano-scale structure and the bimolecular activity. One very good example which served as an inspiration for the present study is the work of Bielinska et al, where DNA–dendrimer complexes were used to transfer oligonucleotides and plasmid DNA into in vitro cell culture system. However, it allows us to directly compare the effect of compaction on the

accessibility of the DNA. Although we are far from the biological system, the same mechanisms should apply though with less parameters to modulate. Another motivation for this study is the growing interest in cell free protein synthesis as described in a recent review. Here the ability to regulate transcription in vitro systems is important. The first objective of the present study is to investigate the compaction of DNA using a cationic polymer or surfactant.

The major binding force for the DNA- dendrimer complex is the electrostatic interaction force **[Fant et al., 2008]**. From the molecular dynamics simulation it in the first few seconds a stable complex will be formed from dendrimer and DNA. A recent experiment study of DNA-dendrimer complexation **[Fant et al., 2008]** suggests that DNA binding with dendrimers can be divided into a "tightly bound DNA" region and a "linker DNA" region. The higher generation of the denderimer allows a higher number of turns of the DNA generations, i.e., the charge ratio between the dendrimer and DNA is maximum. When DNA is mixed with PAMAM dendrimers in electrolyte solution, it undergoes a transition from a semiflexible coil to a more compact conformation due to the electrostatics interaction present between the cationic dendrimer and the anionic polyelectrolyte **[Örberg et al., 2007]**. A recent molecular dynamics simulation showed that despite the DNA rigidity, strong electrostatic interactions cause linear DNA chains to wrap around the dendrimer and penetrate inside it, leading to the formation of a compact complex **[Lee and Larson, 2009].**When a cationic polymer almost or completely neutralizes an anionic DNA, the intermolecular interaction is expected to be purely electrostatic.

1.1 Deoxyribonucleic Acid (DNA)

DNA, or deoxyribonucleic acid, is the hereditary material in humans and almost all other organisms. Nearly every cell in a person's body has the same DNA. Most DNA is located in the cell nucleus (where it is called nuclear DNA), but a small amount of DNA can also be found in the mitochondria (where it is called Mitochondrial DNA or mtDNA) **[Russell,2001]**.

The information in DNA is stored as a code made up of four chemical bases: adenine (A), guanine (G), cytosine (C), and thymine (T). Human DNA consists of about 3 billion bases, and more than 99 percent of those bases are the same in all people. The order, or sequence, of these bases determines the information available for building and maintaining an organism ,which is similar to the way in which letters of the alphabet appear in a certain order to form words and sentences (see figure 1.1). **[Waston and Crick,1953]**.

DNA bases pair up with each other, A with T and C with G, to form units called base pairs. Each base is also attached to a sugar molecule and a phosphate molecule. Together, a base, sugar, and phosphate are called a nucleotide. Nucleotides are arranged in two long strands that form a spiral called a double helix. The structure of the double helix is somewhat like a ladder, with the base pairs forming the ladder's rungs and the sugar and phosphate molecules forming the vertical sidepieces of the ladder. **[Waston and Crick,1953]**.

An important property of DNA is that it can replicate, or make copies of itself. Each strand of DNA in the double helix can serve as a pattern for duplicating the sequence of bases. This is critical when cells divide because each new cell needs to have an exact copy of the DNA present in the old cell **[Berg et al., 2002]**.

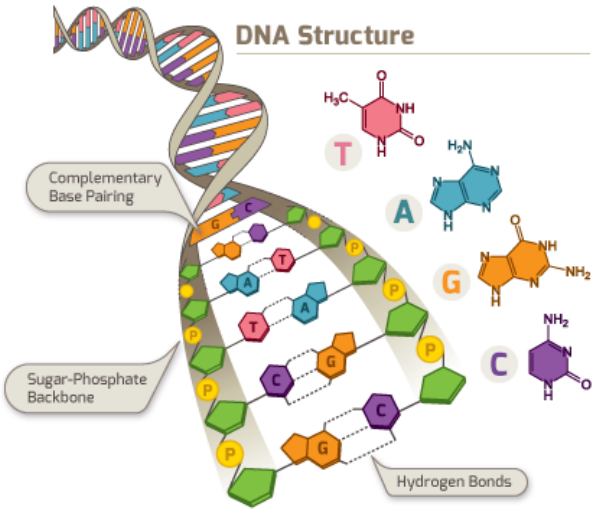

Figure 1.1: DNA contains two strands wrapped around each other in a helix (known as the double helix). Each nucleotide includes 3 parts: a phosphate group, a sugar molecule and one of 4 bases Adenine, Cytosine, Guanine or Thymine. [Thednal, 2015]

1.2 Gene Delivery and the Importance of Charge Inversion

In the last few years gene therapy received significant attention both from the scientific community and from the general public. The development of new techniques for transferring genes into living cells allowed for the potential treatment of several diseases of genetic origin. The central problem of gene therapy lies in the development of safe and efficient gene delivery system. Since both the DNA and the cell membranes are negatively charged, the naked polynucleotides are electrostatically prevented from entering the cells. Furthermore, the unprotected DNA is rapidly degraded by nucleases present in plasma **[Sheridan. C, 2011]**.

Although, much effort has concentrated on viral transfection, non-viral methods have received an increased attention. This is mostly due to the possible complications which can arise from recombinant viral structures, and the consequent risk of cancer. In the non-viral category, the DNA liposome complexes have shown the most promise. Cationic liposomes can associate with the DNA segments, neutralizing or even inverting the electric charge of nucleotides, thus significantly increasing the efficiency of gene adsorption and transfection by cells.

1.3 Dendrimers

Dendrimers are large and complex molecules with very well-defined chemical structures.
From a polymer chemistry point of view, dendrimers are nearly perfect monodisperse (basically meaning of a consistent size and form) macromolecules with a regular and highly branched three-dimensional architecture. They consist of three major architectural components: core, branches, and end groups.

Dendrimers are produced in an iterative sequence of reaction steps, in which each additional iteration leads to a higher generation dendrimer. The creation of dendrimers, using specifically-designed chemical reactions, is one of the best examples of controlled hierarchical synthesis, an approach that allows the 'bottom-up' creation of complex systems. Each new layer creates a new 'generation', which doubles the number of active sites (called end groups) and approximately doubles the molecular weight of the previous

generation. One of the most appealing aspects of technologies based on dendrimers is that it is relatively easy to control their size, composition and chemical reactivity very precisely **[Tiana and Maba, 2012]**.

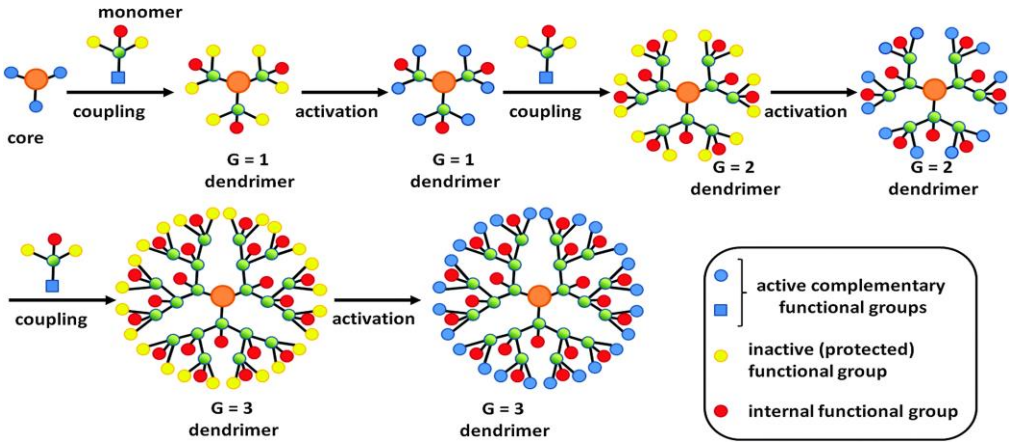

Figure1.2: Dendrimer generations [Marta et. al., 2014].

1.3.1 PAMAM dendrimers

The central component of most new drug delivery systems is a polymeric biomaterial. Among polymeric biomaterials that have been examined as drug carriers is a family of water-soluble cascade polymers named poly amidoamine (PAMAM) dendrimers. PAMAM dendrimers have a unique tree-like branching architecture that confers them a compact spherical shape in solution and a controlled incremental increase in size, molecular weight, and the number of surface amine groups (see Figure 1.3).The potential of PAMAM dendrimers in the controlled drug delivery has been extensively investigated and arises from the high number of arms and surface amine groups that can be utilized to immobilize drugs, enzymes, antibodies, or other bioactive agents. Such conjugates provide a high density of biological agents in a compact system. In addition, PAMAM dendrimers have shown potential as oligonucleotide and gene delivery systems have been used to improve the solubility of sparingly soluble drugs such as piroxicam, and have increased the amount of therapeutic radionuclides delivered to cancer cells **[Parbal et al 2004]**.

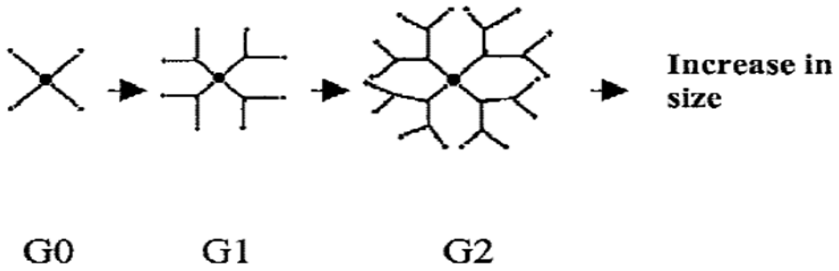

Fig1.3: Schematic drawing of G0, G1, and G2 of starburst dendrimers showing their tree-like branching architecture. The increase in generation number (G0, G1, G2, etc.) results in an incremental increase in size, molecular weight, and number of amine surface groups. [El-Sayed,2001]

To reach the target site, polymeric drug delivery systems including PAMAM dendrimers often must extravagate from the microvasculature across the microvessels endothelium into the surrounding interstitial tissue. The extravasation process of polymeric drug carriers influences the rate of drug delivery to the interstitial tissue, which is the site of action of most drugs. In this study, the extravasation of a series of PAMAM dendrimers across microvascular network endothelium is reported. The unique architecture of PAMAM dendrimers makes them suitable models for studying the influence of a controlled incremental increase in size, molecular weight, and number of amine surface groups on the micro vascular extravasation of polymeric drug carriers. In an attempt to probe the influence of molecular geometry of polymeric drug carriers on their transvascular transport, the extravasation of linear poly ethylene glycol (PEG) molecules is also included and compared to its PAMAM dendrimer counterparts.

The role of pH on packaging and compaction energies attractive and repulsive free energy shows repulsive PAMAM unaffected while attraction linearly with inverse of dendrimer charge **[Dootz et al., 2008].**

1.3.2 Properties of Dendrimers

1.3.2.1 Monodispersity and Polyvalency

The monodispersity of dendrimer - dendritic polymers that can be constructed with a well-defined molecular structure, unlike the linear polymers, has been extensively verified by gel electrophoresis and transmission electron microscopy (TEM) **[Jackson et al., 1998].** The

convergent growth process permits the purification process at each step of the synthesis which gives the monodisperes molecules so that convergently produced dendrimers are probably the most precise synthetic macromolecules that exist today **[Tomalia, 2005]**. However, the divergent method is remarkably monodisperse for generation (G = 0 – 5) **[Tomalia, 1993]**. Monodispersity offers researchers the possibility to work with well-defined scalable sizes. This property is useful for applications such as the synthesis of container molecules. Polyvalency of dendrimers provides many interactions as they coordinate to materials. Polyvalency shows the outward presentation of reactive groups on the dendrimer nanostructure exterior, it depends upon which functional groups are attached to the tip of a dendrimer's branches. These functional groups can participate in multiple interactions with receptors on biological structures like cell membranes and viruses **[Halford, 2005]**.

1.3.2.2 Nanoscale size and shape

Dendrimers are referred as artificial proteins **[Svenson and Tomalia, 2005].** Within the PAMAM dendrimer family, the diameter of the generation (G1– G10) with ethylenediamine core increases from 1.1–12.4 nm **[Cheng et al., 2008]**. The shape of dendrimer is very important, as it allows to define placement of functions not only on dendrimer surface but also inside the dendritic scaffold. The PAMAM dendrimer of lower generation (G0–G3) with ethylenediamine core have ellipsoidal shapes, whereas the PAMAM dendrimer of higher generation (G4–G10) have roughly spherical shapes **[Cheng et al., 2008]**.

1.3.3 Applications of Dendrimers

Current research is being performed to find ways to use dendrimers to deliver genes into cells. The ability to deliver pieces of DNA to the required parts of a cell without damaging DNA, also to maintain the activity of DNA during dehydration is a challenge since their introduction in the mid-1980s. This class of dendrimer architecture has been a prime candidate for host guest chemistry **[Tomalia et al., 1990]**. Dendrimer may be used as drug delivery either the drug is coordinated to the outer functional groups via ionic interactions, or the dendrimer encapsulate a pharmaceutical drug and this encapsulation increases with

dendrimer generation. The use of dendrimers as unimolecular micelles was proposed by Newkome in 1985 **[Newkome et al., 1985]**. This analogy highlighted the utility of dendrimers as solubilizing agents since the majority of drugs available in pharmaceutical industry are hydrophobic in nature and this property in particular creates major formulation problems and the dendrimer can be used as drug delivery **[Prajapati et al., 2009]** and target specific carrier **[Kukowska-Latallo et al., 2005]**. Dendrimers have been used for the encapsulation of hydrophobic compounds and for the delivery of anticancer drugs.

1.4 Previous studies

1.4.1 Experimental studies

The binding interaction between salmon sperm DNA of 2000bp (L = 680nm) and PAMAM dendrimers of G4 has been investigated. The results based on dynamic light scattering (DLS) and steady-state fluorescence spectroscopy have made it possible to propose a binding model which is cooperative **[Örberg et al., 2007]**. In a recent experimental study carried out by using cryo-TEM, dynamic light scattering (DLS) and fluorescence spectroscopy **[Ainalem et al., 2009]** showed that the morphologies of the aggregate formed between DNA and PAMAM dendrimers of different generations are affected by dendrimer size and charge at low charge ratio ($r_{charge} < 1$) in dilute solution. At such conditions the process is cooperative and well-defined structured aggregates are formed for lower dendrimer generations. The smaller sized dendrimers (G1 and G2), which have a lower total charge per molecules, allow the formation of well-structured rods and toroids. In contrast, globular and less defined aggregates are formed with higher generation dendrimers. The dendrimer binding to DNA has also been found to be sufficiently strong. For increasing charge values, the fluorescence emission intensity gradually decreases. This indicates that the amount of free DNA decreases for increased dendrimer concentrations. Ainalem and co-workers assumed that all dendrimers interact with DNA, for low charge values and the mean resulting numbers of dendrimers per condensed DNA chain of 4331bp are then 318, 16 and 5 for the G2, G6 and G8 of dendrimers respectively. According to the relation $r_{charge} = N_{exp} * Z_{dend} / Z_{DNA}$, these values correspond to mean charge ratios of 0.47 for G2, 0.59 for G6 and 0.61 for G8. The calculated compositions of the dendrimers-DNA aggregate can be compared to the number of 35 for

G4 dendrimers that were found per 2000bp (L = 680nm) salmon sperm DNA, which corresponds to a charge ratio of 0.56 in the dendrimer/DNA aggregates.

A recent experimental study was performed by Carnerup and co-workers **[Carnerup et al., 2011]**. Where they studied the condensation of DNA by dendrimer of generations G1, G2, G4, G6, and G8 as a function of salt concentration, and they observed there was an increase in the size of the aggregate formed by lower generations (G1, G2, and G4) when the salt concentration increased. As more rod-like aggregates are observed, whereas for higher generations there was no change in the size i.e., such aggregate formed by condensation of DNA by dendrimer of G8 is insensitive to salt concentration. This is attributed to the higher charge of higher generation which is more effective to form neutralized aggregates that show the micrographs for different morphologies at salt concentration 150 mM of NaBr compared with for salt concentration of 10mM NaBr, where both have scale bars of 100 nm.

Ainalem observed that G4 dendrimer is more efficient in DNA compaction than hexadecyltrimethyl ammonium bromide (CTAB) due to high charge +64 in G4 dendrimer **[Ainalem et .al, 2014]**

1.4.2 Computer Simulation Studies

The complexation of a PAMAM dendrimer with an oppositely charged LPE has motivated many simulation studies which aimed to understand the atomistic details of the process. Luylin **[et al., 2005]** performed Brownian dynamics computer simulations of complexes formed by charged dendrimer and oppositely charged linear polymer chain of different degrees of polymerization (different numbers of monomers on the chain N_{ch}). They showed that the monomers of the linear chains with N_{ch} equal to the number of dendrimer's terminal charged groups are located very close to these terminal groups. For longer chains the total number of the chain monomers adsorbed onto a dendrimer exceeds the number that is necessary to neutralize dendrimer´s charge. The overcharging phenomenon was observed. A recent Molecular Dynamic (MD) simulation study, Luylin **[2008],** showed that the maximum of the LPE chain adsorption occurs at some critical length of LPE chain. The

first order phase transition from completely coiled conformation to the conformation with released tails takes place upon increasing the linear-chain length above the critical length. The one-long-tail conformation becomes energetically preferable. Larin and co-workers **[Larin et al., 2009]** studied the structural properties of the complexes formed by two macroions and a LPE chain. They found that the dependence of Nonmonotonic of the linker size on the LPE chain length was observed.

More advances in molecular dynamics simulation methodologies and computational power performed such as the coarse-grained (CG) simulations. Tian and Ma **[Tian and Ma, 2010]** employed extensive coarse – grained molecular dynamic simulation to study the influence of rigidity of the LPE chain on dendrimer – LPE complexes. They found that as a soft nanoparticle. The change in size and shape of dendrimer depends on the Bjerrum length of the medium and the condensed LPE chain monomers have an additional possibility for the localization near the opposite charge inside the layer.

1.4.3 Theoretical Studies

The first theoretical models on sphere – LPE chain complexation were presented in 1999. Park **[1999]**considered a semiflexible and highly charged PE chain and showed that counterion release leads to overcharging. Mateescu and co-workers **[Mateescu et al., 1999]** considered the interaction between a spherical macroion of charge Z_e and an oppositely, highly charged polyelectrolyte of charge $-N_e$. They showed that, for $N > Z$, the amount of collapsed polyelectrolyte can be bigger than that required to neutralize the macroion, *i.e.* the macroion can be overcharged. The overcharging increases with the diameter of the macroion. The predictions of this model are compared with Monte Carlo Simulations. Netz and Joanny **[Netz and Joanny, 1999]** studied the interaction of a charged semiflexible polymer with an oppositely charged hard sphere. Both the effect of salt concentration and the stiffness of the polymer are taken into account. They showed that for intermediate salt concentration and high enough sphere charge a strongly bound complex obtained where the polymer completely wraps around the hard sphere. The complex may or may not exhibit charge reversal, depending on the sphere charge and slat concentration. In the case of low salt , the regime is dominated by the polymer-polymer repulsion, the polymer partially

wraps around the sphere, and the two polymer arms extend parallel and in opposite directions from the sphere. Whereas in high salt regime they found bent solution, and the salt dependence of the wrapping transition for large salt concentrations agree with experimental results for the complexation of synthetic polyelectrolytes with charged colloids. Nguyen and Shklovskii **[Nguyen and Shklovskii, 2001]** studied the complexation of a polyelectrolyte with an oppositely charged spherical macroion modeled impenetrable sphere, for both salt free and salty solutions. They showed that when a polyelectrolyte winds around the macroion, its turns repel each other and form an almost equidistant solenoid. Nguyen and Shklovskii concluded that this correlation of turns lead to the charge inversion, and the charge inversion becomes stronger with increasing concentration of the salt. This analytical study agrees with Monte Carlo simulation results.

Schiessel and co-workers **[Schiessel et al., 2001]** considered complexes formed between positively charged macroion and a persistence LPE. They studied first the case of complexation with a single hard sphere and calculated the wrapping length of the chain. Then they extended their consideration to complexes of many wrapped spheres. (See appendix A).

Schiessel and co-workers showed how the resulting complexes depend on the persistence length of the linear polyelectrolyte, the salt concentration, the size and charges of the chain and the macroions **[Schiessel et al., 2001]**. In the same frame of this analytical model Qamhieh and co-workers **[Qamhieh et al., 2011]** inserted minor modifications to the model. They studied the net charge of the complex conformed by dendrimer of G4 complexes with semiflexible LPE chain of two lengths, and how much the LPE chain wrapped around the dendrimer and the number of dendrimers in the aggregate. Throughout the analytical study, the term (complex) refers to the interaction between a single ion-penetrable sphere representing dendrimer and segment of linear polyelectrolyte (LPE) representing DNA molecule that wrapped around dendrimer. And the term (aggregate) refers to the interaction between a multiple of dendrimers and the Whole DNA molecule length.

They concluded that dendrimers are likely to contract upon interaction with oppositely charged LPE. For this reason Qamhieh and co-workers recommend to replace the complexation of semiflexible LPE chain with the impenetrable sphere by a soft sphere. Qamhieh and co-workers **[Qamhieh et al., 2011]** extended this analytical study to include the interaction between semiflexible LPE chain and oppositely charged dendrimer of generations G2, G4, G6 and G8. One length of LPE used 4331bp. They found that the number of turns of LPE around dendrimer increases with dendrimer generation, and the net charge of the aggregates is independent of dendrimer size when it contracts especially for a higher generation.

Larin et al., [2010] studied the structure of the complexes formed by two dendrimers and an oppositely charged LPE. In these systems, dendrimers are strongly overcharged by the adsorbed LPE monomers and the maximum degree of the overcharging is close to that in complexes formed by one dendrimer and LPE. The overcharging degree does not decrease significantly in the 2g3 complexes, after the maximum of chain adsorption is reached. In contrast to the complexes comprised by a single dendrimer and LPE, linker formation is due to the increase of the LPE in the complexes and the linker size depends on the LPE length nonmonotonously, in spite of the rather narrow interval of simulated parameters and model potentials (absence of hydrogen bonding, Debye-Hu¨ckel approximation for the electrostatic interactions, etc.) which may be far from the realistic biological situation. We believe that our findings provide new insights for dendrimer-LPE complexation. The obtained simulation results are in qualitative agreement with the predictions of the developed correlation theory for complexes formed by two spherical macroions and a flexible polyelectrolyte chain.

Typical snapshots of complex formed by two dendrimers are shown in Figure 1.4. It is seen that the configuration of a complex strongly depends on (L). We recognize in Figure 1.4 the region of chain lengths where dendrimers are close to each other and form a joint macroion without linker (Figure4a). At large L, the linker between dendrimers exists (Figure 4b and c).

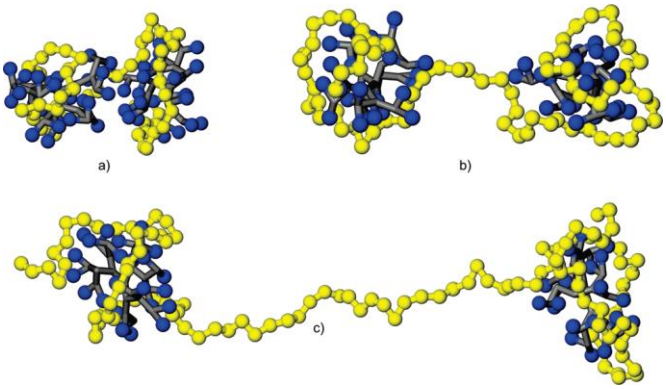

Figure 1.4: Snapshots for equilibrated 2g3 complexes with different values of the LPE length(L) , a) 55 , b) 70,and c) 110,[Larin et al.,2010].

The role of pH on packaging and compaction energies attractive and repulsive free energy shows repulsive PAMAM unaffected while attractions linearly with inverse of dendrimer charge.

1.5 Statement of the Problem

Through our study we described dendrimer as ion penetrable sphere (soft sphere) as **Qamhieh and Abu Khaleel (2011)**, where the ions can penetrate inside the dendrimer, (see figure 1. 5). They did their study for simple model DNA-Dendrimer, while we investigate the complexation between DNA and multi- dendrimers of different generations (G1-G2-G3-G4-G6-G8). In our study we investigate the effect of some factors, like salt concentration, persistence length(l_p), dendrimer generation size, pH of the solution, and the strength of electrostatic interaction.

Figure1.5: Graphic of (a) hard sphere model, and (b) a soft sphere (ion- penetrable) model.

Chapter TWO

The Theoretical Model

Chapter Two

2.1 Introduction

In this study we used a penetrable model for the complexation of DNA with dendrimer which has been developed by **Qamhieh et al. (2009),** and used all the parameters into this model to find out its impact on the complex.

2.2 Analytical model of the system:

Qamhieh and co-workers considered complexes formed between soft (ion penetrable) sphere of radius R and charge Z, represent the dendrimer and the DNA as a linear polyelctrolyte (LPE) chain of l_p persistence length, of radius $a = 1\,nm$, length $L >> R$ and the charge density of LPE is $\lambda = -e / b$, where b is the axial spacing between charges on the chain. The sphere and the LPE chain are placed in 1:1 salt solution in a system characterized by Bjerrum length $l_B = e^2/\varepsilon k_B T$, where $k_B T$ is thermal distance, ε is dielectric constant of the medium, k_B is Boltzmann constant, T: absolute temperature,and a Debye screening length is $\kappa^{-1} = (8 c_s \pi l_B)^{-1/2}$ where c_s is the salt concentration.

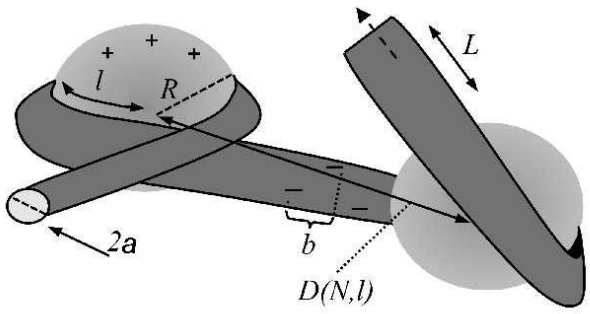

Figure 2.1: Proposed binding model between DNA of contour length *L*, radius *a*, and distance between negative charges *b* and G4 PAMAM dendrimers modeled as hard spheres of radius *R*. The DNA is shown to wrap around the dendrimer with the length of the wrapping part equal to *l*, and a distance between the centers of two neighboring dendrimers, *D* (*N*, *l*). The model is in accordance with the cooperative binding model proposed by Örberg on co-workers (Örberg et al., 2007).

2.3 Complexation of a chain with multiple spheres:

Schiessel model for electrostatic complexation assumes that the total free energy of the system consisting of one dendrimer and one DNA segment can be expressed as a sum of four contributions; see Eq. (A.1) in appendix A.

$$F(l) = F_{compl}(l) + F_{chain}(L-l) + F_{compl-chain}(l) + F_{elastic}(l) \qquad 2.1$$

Where *l* is the length of the DNA molecule wrapped around the sphere (dendrimer), and the remaining chain is of length (L-*l*).

The electrostatic charging of free energy of spherical penetrable sphere complex from the model is:

$$F_{compl}(l) \cong \frac{3Z^2(l) l_B k_B T}{8\pi(kR)^2}\left[\cosh(kR) - \frac{\sinh(kR)}{kR}\right]\frac{e^{-kR}}{R} \qquad 2.2$$

Eq. (2.2) implies that $F_{compl}(l)$varies quadratically as$(Z - l/b)^2$. There is special length $l_{iso} = bZ$ such that $Z(l = l_{iso}) = 0$. Simply invoking the principle of charge neutrality would lead to expect that the total free energy is minimized for $l \approx l_{iso}$, where l_{iso} is the isoelectric chain length needed to compensate the charge of the porous sphere.

The total entropic free energy of the remaining chain is:

$$\mathrm{F_{chain}(L-l)} \cong \frac{\mathrm{k_B T}}{\mathrm{b}} .\Omega(\mathrm{a}).(\mathrm{L-l}) \qquad 2.3$$

where $\Omega(\mathrm{a})$: is the entropic cost.

And the energy between the complex and the free segment of the LPE is:

$$F_{compl-chain}(l) \cong \frac{3Z(l) l_B k_B T}{4\pi(kR)^2}\left[\cosh(kR) - \frac{\sinh(kR)}{kR}\right] \times \left[\ln(r) - \sum_{n=0}^{\infty}\frac{(-1)^n}{(n+1)!.(n+1)} .(kR)^{n+1}\right]\Big|_R^{L-l} \qquad 2.4$$

The last term which corresponds to the elastic free energy is:

$$F_{elastic}(l) \cong \frac{k_B T l_B}{R^2}\, l \qquad 2.5$$

Substituting equations (2.2-2.5) in 2.1 will give us the total energy in one dendrimer with DNA molecule.

The total free energy for a system consisting of one LPE chain and N number of spheres (see Eq. (A.9) in appendix A) can be expressed as:

$$F(l,N) = NF(l) + F_{int}(N,l) \qquad 2.6$$

The second term in Eq. (2.6) represents the repulsive electrostatic interaction free energy between hard spheres. Also, this term has to be modified to represent the electrostatic interaction free energy between penetrable spheres where $F_{int}(N,l)$ represent the repulsive electrostatic interaction free energy between penetrable spheres.

Ohshima found the electrostatic interaction free energy between two ion – penetrable spheres (see Eq. (B.28) in appendix B). Each of charge Z_e is as the following:

$$F_{int}(N,l) = \frac{9Z^2(l)k_BTl_B}{8\pi\,\varepsilon(kR)^4}\left[\cosh(kR) - \frac{\sinh(kR)}{kR}\right]^2 \frac{e^{-kD}}{D} \qquad 2.7$$

For the case of the interaction between complexes, each of charge $Z(l)$e, using Eqs.(2.3), (2.4) and (2.7). Then, the interaction free energy can be obtained by summing over the electrostatic repulsion between all complexes within one chain. We get

$$F_{int}(N,l) = \frac{9Z^2(l)k_BTl_B}{8\pi\,\varepsilon(kR)^4}\left[\cosh(kR) - \frac{\sinh(kR)}{kR}\right]^2 \times \sum_{i=1}^{N-1}\left[\left[\frac{N-i}{i}\right]\frac{e^{-kD(N,l)}}{D(N,l)}\right] \qquad 2.8$$

Where $(D\ (N,l))$the center-to-center distance between two complexes next to each other which equals to $(L - Nl + 2NR)/N$, is small at very low ionic strength. This interaction energy worths nothing that this term will be small if the charge of complex is close to neutral.

For simplification we write

$$A = \cosh(kR) - \frac{\sinh(kR)}{kR} \qquad 2.9$$

Substituting the equations 2.2, 2.3, 2.5, 2.7 in equation 2.6

$$\frac{F(N,l)}{k_B T} = \frac{3NZ(l)l_B A}{4\pi(kR)^2}\left[\frac{Z(l)e^{-kR}}{2R} + \frac{1}{b}.\int_R^{L-Nl}\frac{e^{-kR}}{r}dr + \frac{3Z(l)A}{2N(kR)^2}\sum_{i=1}^{N-1}\binom{N-i}{i}\frac{e^{-kD}}{D}\right] \qquad 2.10$$
$$+\frac{1}{b}.\Omega(a).(1-\xi^{-1}).(L-Nl) + \frac{Nl_b}{2R^2}l$$

This equation derived by **Qamhieh et al., (2009)**, represents the total energy of the system in units of $k_B T$, and used for investigation of the behavior of the dendrimer during the interaction with LPE **[Qamhieh et al., 2009].**

Chapter Three

Results and Discussions

Chapter Three: Results and Discussions

3.1 Results of electrostatic free energy interaction of the complexation between LPE chain and multi- penetrable spheres:

The electrostatic interaction free energy for a system of LPE chain and an oppositely charged sphere has been studied by the ***penetrable sphere model***. The LPE chain modeled DNA molecule of $88\,bp$, and penetrable sphere of charge $Z = 64$ and $Z = 24$, radius $R = 2.25nm$ and $R = 3.2nm$ for PAMAM dendrimer of generation 4 (G4) and generation 3 (G3) respectively with a different number of dendrimer ($N = 1, 2, 3, 4\ and\ 5$), at concentration of 1:1 salt solution NaBr corresponds to Debye screening length of 3nm and Bjerrum length of 0.71nm at room temperature.

The optimal wrapping length (l_{opt}) of LPE chain which has been wrapped around dendrimer can be found by taking the first derivative of total free energy equation for the penetrable sphere model (Eq.2.10) with respect to the wrapping length l, then equating it to zero. The calculation results of the parameters in equation 2.10 for G3 and G4 are summarized in table 3.1. It can be seen that the optimal DNA wrapping length increases for higher dendrimer generation, D' which is the length of the DNA linking two neighboring dendrimer generation increases.

	G3					G4				
Number of dendrimer	**N=1**	**N=2**	**N=3**	**N=4**	**N=5**	**N=1**	**N=2**	**N=3**	**N=4**	**N=5**
l_{opt}	28.32	14.3	10.8	7.2	5	28.7	14.7	11	7.7	5.7
$Dif(nm)$	24.24	10.22	6.72	3.12	0.92	17.8	3.8	0.12	-3.18	-5.18
Z^*	-142.6	-60.1	-39.5	-18.4	-5.4	-104.8	-22.5	-0.71	18.71	30.5
Z^*/Z	-5.9	-2.5	-1.65	-0.77	-0.2	-1.64	-0.35	-0.011	0.29	0.48
$D(N,l)(nm)$	8.08	7.1	6.1	6.7	7.4	5.8	4.8	3.5	4.3	4.8
$D' = D - 2R\ (nm)$	1.68	0.7	0.3	0.3	1	1.3	0.3	1	0.02	0.3

Table 3.1: Analytical results for the parameters calculation of 1, 2, 3, 4, and5 of G3 and G4 with contour length $L = 30\ nm$.

Figure 3.1 shows the relation between the free energy in units of K_BT of 1, 2, 3, 4, and 5 (a)G4 ,(b)G3 – LPE chain complex **(**Eq. (2.2)) as a function of the wrapping length, which varies quadratically $F_{comp}\ \alpha\ Z^2\ (l)$. The free energy will increase as the number of dendrimers increases and passes through l_{iso} at which the complexe is electrostatically

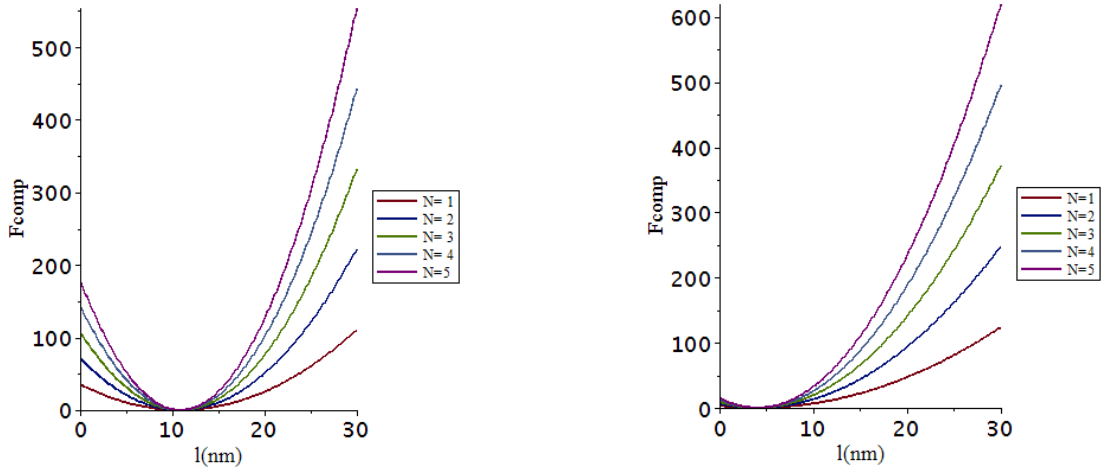

(a) **(b)**

Figure 3.1: Electrostatic charging free energy in units of k_BT of 1, 2, 3, 4, and 5 (a) G4 (b) G3 – LPE chain complex as a function of the wrapping length.

Figure3.2 shows the electrostatic free energy in units of K_BT between 2, 3, 4, and 5(a) G4, (b) G3 – LPE chain is complex and free chain of length $(L-l)$ as a function of the wrapping length (Eq (2.4)). Before the optimal length , it is an undercharged complex and then it decreases since the charge of chain is dominant for single dendrimer. For multi dendrimers it increases again which results in an increase in dendrimer numbers which will lead to a sharper increase in energy

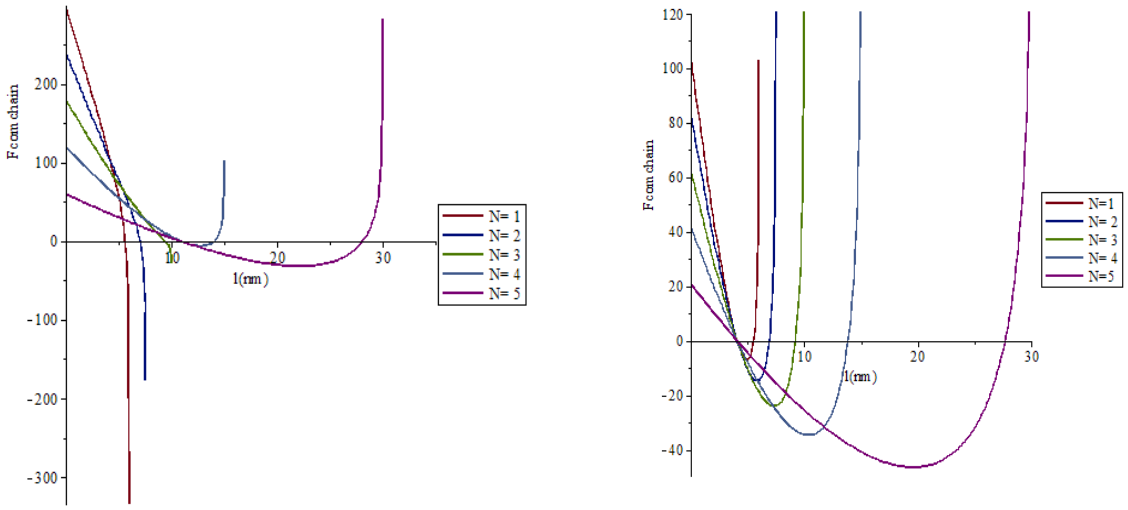

(a) **(b)**

Figure 3.2: Electrostatic interaction free energy in units of k_BT between 2, 3, 4, and 5(a) G4, (b) G3 – LPE chain complex and free chain of length $(L-l)$ as a function of the wrapping length.

Figure 3.3 shows the electrostatic interaction free energy between multi complexes as a function of the wrapping length (Eq2.7) . The energy increases as the complexes number increases and the neutralization occurred when $l = l_{iso}$. At a higher dendrimer number , it will be sharper energy increase and the interaction free energy is zero for both G3 and G4.

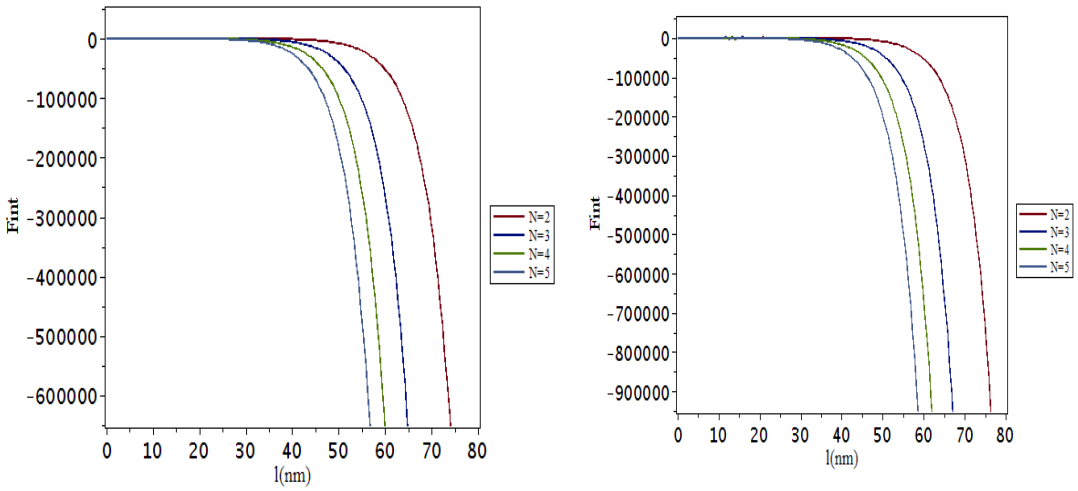

(a) **(b)**

Figure 3.3: Electrostatic interaction free energy in units of k_BT between 1, 2, 3, 4, and 5 (a)G4, (b)G3 – LPE chain complexes as a function of the wrapping length.

Figure 3.4(a) represents the total electrostatic free energy (Eq (2.10)) for G4 and Figure 3.4(b) for G3. The electrostatic free energy minimized to each other, but in G4 it is minimized to a negative charge and neutralization occurred when the number of dendrimer increases.

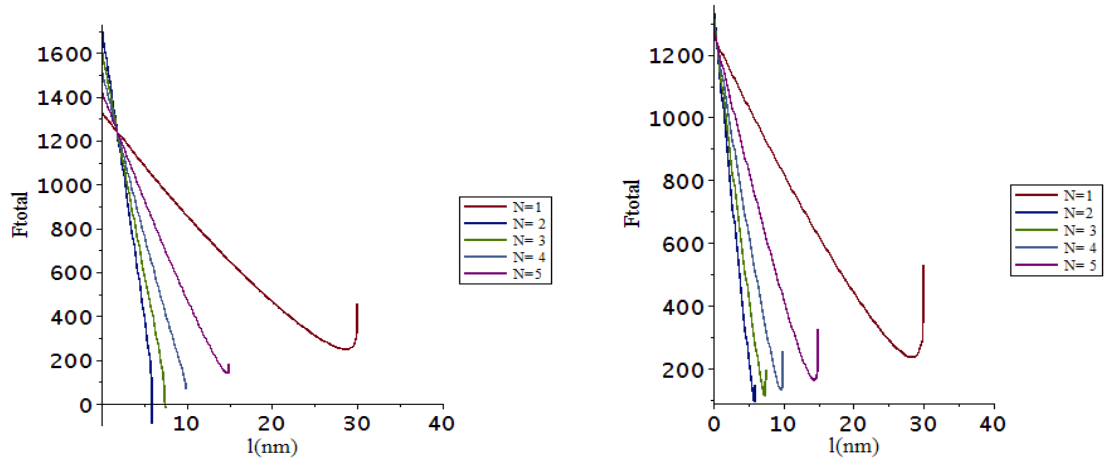

(a) **(b)**

Figure 3.4: The total electrostatic free energy in units of k_BT of 1, 2, 3, 4, and5 (a) G4, (b) G3 – LPE chain complexes as a function of the wrapping length.

3.2 Effect of Dendrimer Size Generation on Optimal Length Condensed on PAMAM Dendrimer:

To cover the effect of a different generation on the complex formation, we took multi-PAMAM dendrimer of a different generation (G3 and G4) to compare the change in behavior of each one when the charge and radius change for each generation of dendrimer, at a constant parameter of the complexation. The system is composed of the flexible LPE chain of persistence length $lp = 3nm$, charge spacing of the chain is $b = 0.17nm$, and length $L = 680\,nm$, and the penetrable sphere model at 1:1 salt concentration corresponding to Debye screening length (DSL) of 6nm, have been studied at different generation dendrimers using the penetrable sphere model with PAMAM dendrimer.

Figure 3.5 shows that the optimal DNA wrapping length around the two dendrimers increased for higher dendrimer generation and higher number of dendrimer. Moreover it shows that the number of DNA turns around a dendrimer increases with the dendrimer size or generation and number of dendrimers. This finding is in agreement with experimental studies by **(Ainalem et al. and Carnerup et al.)** reporting on dendrimer/DNA aggregate morphologies. It should also be mentioned that the shape of the dendrimers changes with generation and higher generation is typically more spherical than the lower generation that has a more disc-like shape **(Lee et al., 2002, .Paulo et al., 2007,).**

The highly ordered rods and toroids found that low generation dendrimers can be attributed to the fact that the DNA wraps less than one turn around the dendrimer. Consequently, the disordered globular structures that appear for high generation

dendrimers, is likely a consequence of the wrapping of DNA in several turns around these dendrimers (see Table 3.2).

generation	$lopt$	$lopt\ /2\pi R$	Z^*_{compl}	Overcharging degree $(\ lopt - liso)\ /\ liso$
G1	87	9.2	-505.8	84.3
G2	183	13.2	-1052.5	88.7
G3	417	20.7	-2426	101.1
G4	580	23.1	-3363.8	70.1
G6	643.3	27.3	-3423.8	18.7

Table 3.2: The overcharging degree of Two dendrimer of different size generation by DNA of 2000bp (L=680nm).

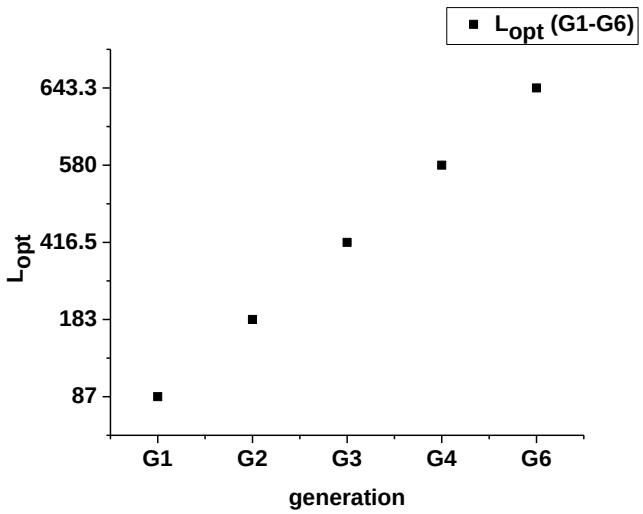

Figure 3.5: Effect of different generation of two dendrimer on optimal wrapping length around LPE chain of persistence length $lp = 3nm$, charge spacing of the chain is $b = 0.17nm$, and length $L = 680\ nm$, and the penetrable sphere model at 1:1 salt concentration corresponding to Debye screening length (DSL) of 6nm.

3.3 Effect of Bjerrum Length on PAMAM Dendrimer – LPE Complex Conformation

The flexible LPE chain of persistence length $lp = 30nm$, of the total length $140bp$, corresponds to Debye screening length 6nm, and penetrable sphere of charge $Z = 24$ and $Z = 64$ and radius $R = 3.2nm$ and $R = 2.25$ representing PAMAM dendrimer of generation 3 and generation 4.

Figure 3.6 shows the results of the effect of the Bjerrum length on the wrapping length, which have been calculated by the penetrable sphere model. Bjerrum length is presented here as a dimensionless number throughl_B/b, in generations G3 as it is shown. The ratio of l_B / b increases, i.e... When the attractive electrostatic interactions increase, the optimal wrapping length increases. As the number of dendrimers increases, the optimal wrapping length increases. Bjerrum length indicates the electrostatic interaction strength its increase will lead to stronger interaction and so the increase of l_{opt} the l_{opt}value in

G4 is more than the l_{opt} value in G3 at the same number of dendrimer. For example, at $N = 2$, the maximum l_{opt}value reaches $53\ and\ 60$ for G3 and G4 respectively.

Figure 3.7 shows the effect of the Bjerrum length on the linker formed between LPE chain G3 and G4 complexes with a different number of dendrimers($N = 2.3.4.5$). Also as dendrimers number increases, the linker length decreases due to a stronger electrostatic interaction and the effect of l_B/b slightly decreases the linker length. This will lead to increase the adsorbed monomers as the number of dendriners increases.

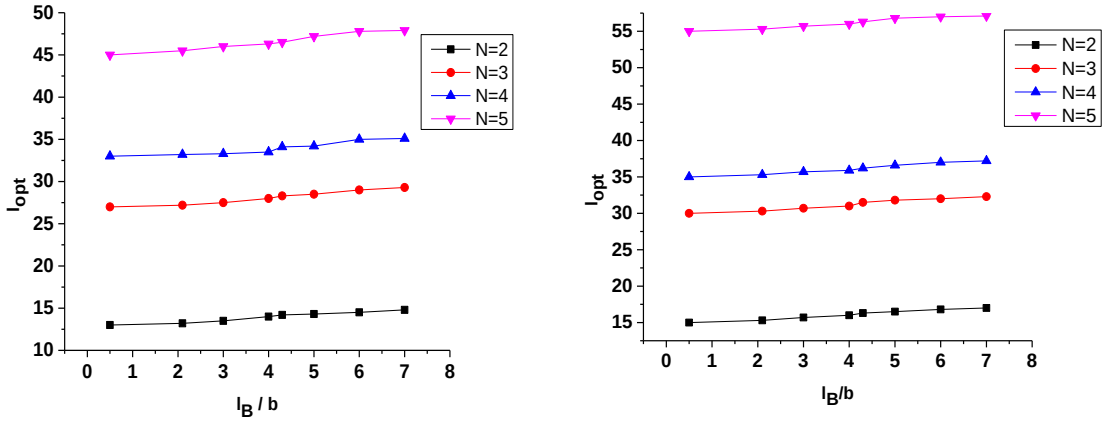

(a) **(b)**

Figure3.6: The effect of the Bjerrum length on the wrapping length (a) G3 (b) G4 with different number of dendrimer,($N = 2.3.4.5$).

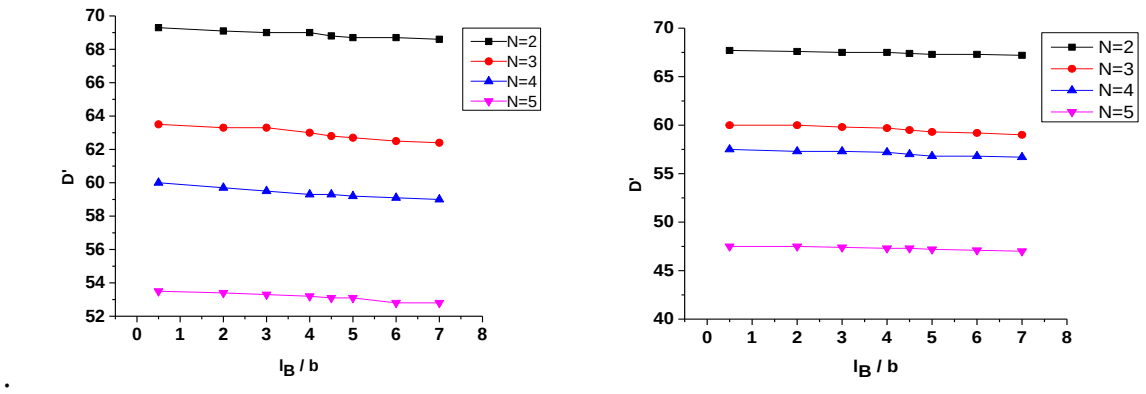

.

(a) **(b)**

Figure3.7: The effect of the Bjerrum length on the linker formed between LPE chain – 2, 3, 4, and 5(a) G3 and (b) G4 complexes.

3.4 Effect of Salt Concentration on Multi-PAMAM dendrimer - LPE Complex Conformation:

The LPE chain modeled DNA molecule of 587 bp, and the penetrable sphere of charge $Z = 24$ and radius $R = 3.2nm$ representing PAMAM dendrimer of generation 3(G3), for different concentrations of 1:1 salt solution at room temperature which gives 0.71nm of Bjerrum length.

Figure 3.8 shows the fraction of condensed monomers of LPE chain on ammonia cored PAMAM Dendrimer G3 with a different number of dendrimer (N=2, 3, 4, 5). From this figure, upon increasing the concentration of salt , the LPE chain becomes more wrapped around dendrimer where the saturation in the number of the condensed monomers of LPE chain at larger salt concentration is due to the finite and fixed length of the LPE chain. We have two terms in the total free energy equation (Eq. (2.10)) that tend the LPE

chain to resist the wrapping around dendrimer namely, the mechanical bending free energy and the

electrostatic repulsive free energy between the chain monomers. The latter loses its importance with an increase of salt concentration. These repulsions are balanced by the electrostatic attraction between dendrimer – LPE chain complex, which favors the bending of LPE chain in order to wrap around dendrimer **[Kunze and Netz, 2002].** The dendrimer is always overcharged, that is, the condensed monomers of the LPE chain on dendrimer exceed the dendrimer charge and the overcharging degree becomes larger at a higher salt concentration. In other words, when the Debye screening length becomes in the order of the spacing between LPE chain monomers, our study is in agreement with the theoretical study **[Boroudjerdi et al., 2011]** and computer simulation study **[Luylin et al]**. Additionally, the ratio l_{opt}/L increases when N increases at the same concentration of salt.

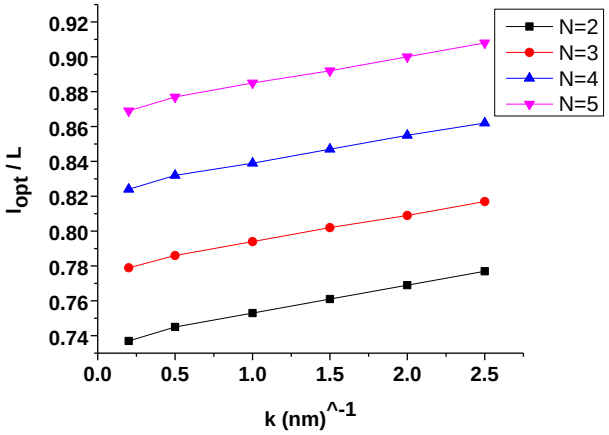

Figure 3.8: The fraction of condensed monomers of LPE chain on 2,3,4,and 5 PAMAM Dendrimer G3 of charge $Z_{dend} = 24$ as a function of concentration of 1:1 salt solution, a constant length of flexible LPE equals to $L = 200nm$, of persistence length equals to 3nm.

Figure 3.9 shows the fraction of the condensed monomers of LPE chain as a function of 1:1 salt concentration for a system of one positively charged dendrimer of Gx . The charge and radius of dendrimers, as shown in Table 3.3. Table 3.4 shows the optimal

wrapping length of LPE chain around dendrimers of different generations, G2, G4, G6 and G8. In Figure 3.8, the fraction of the condensed monomers of LPE chain on dendrimer is displayed. It is shown that for the complex formed by lower generation, namely, G2, and G4 upon increasing the salt concentration ,the fraction of the condensed monomers on dendrimer increases considerably whereas for higher generations G6 and G8 , the fraction of the condensed monomers doesn't change significantly which means that the aggregate formed from the complexation between LPE chain and dendrimer of higher generations seemed to be more neutralized because more and more of DNA charges are being more neutralized by higher generations. This trend is found in agreement with recent experimental study **[Carnerup, et al., 2011].**

Dendrimer	G2	G4	G6	G8
Z (charge)	16	64	256	1024
$R\ (nm)$	1.45	2.25	3.35	4.85

Table 3.3: Charge and Radius of Dendrimer.

Salt concentration (mM)	$l_{opt}(nm)$			
	G2	G4	G6	G8
10	786	808.1	837.1	923.3
30	787.9	812.6	838.7	923.4
50	793.2	814.5	839.1	923.2
100	793.5	816.7	839.4	923
120	794	817.1	839.4	923
150	795	817.4	839.5	922.9
200	796	817.9	839.4	922.9

Table 3.4: Analytical model results for the interaction between two Gx dendrimer and the longer DNA ($4331bp$), the dendrimer is considered to be a penetrable sphere of radius R.

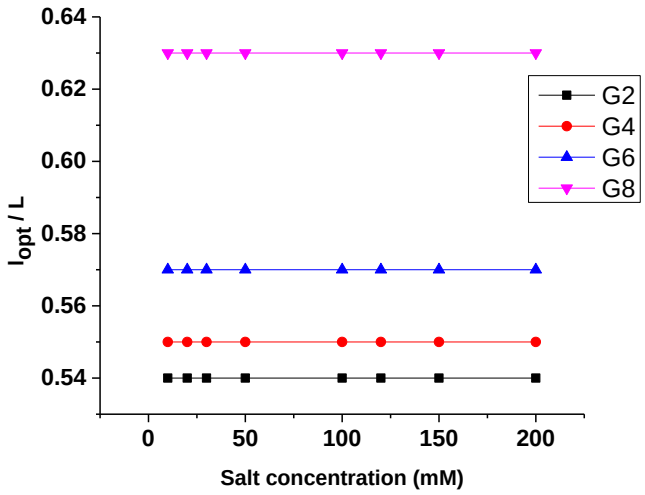

Figure 3.9: The fraction of the condensed monomers of LPE chain as a function of 1:1 salt concentration for a system of one positively charged dendrimer of Gx and a appositively charged semi flexible LPE chain of persistence length $l_p = 50nm$ representing DNA of 4331bp ($L = 1472.5nm$), the dendrimer is considered to be penetrable sphere of radius R.

3.5 Effect of the Length of the LPE Chain on the Linker:

The complexation between flexible LPE chain and an oppositely charged sphere has been studied at variant chain lengths L. The sphere modeled as PAMAM dendrimer G3 of charge $Z = 24$ and $R = 3.2nm$ and G4 of charge $Z = 64$ and $R = 2.25$, LPE chain of persistence length $l_p = 50nm$ and $100nm$ of Debye screening length.

To get the stable LPE chain of multi dendrimers (1, 2, 3, 4, and 5) complexes, the total free energy was minimized. As it is shown in Fig 3.10, the configuration of the complexes depends on the length of the LPE chain. The wrapping length depends on the length of the LPE chain. As the number of dendrimer increases, the number of linker increases and the optimal wrapping length decreases, Result are agreement with results of Brownian Dynamic (BD) simulation [**Larine et al., 2010]**.

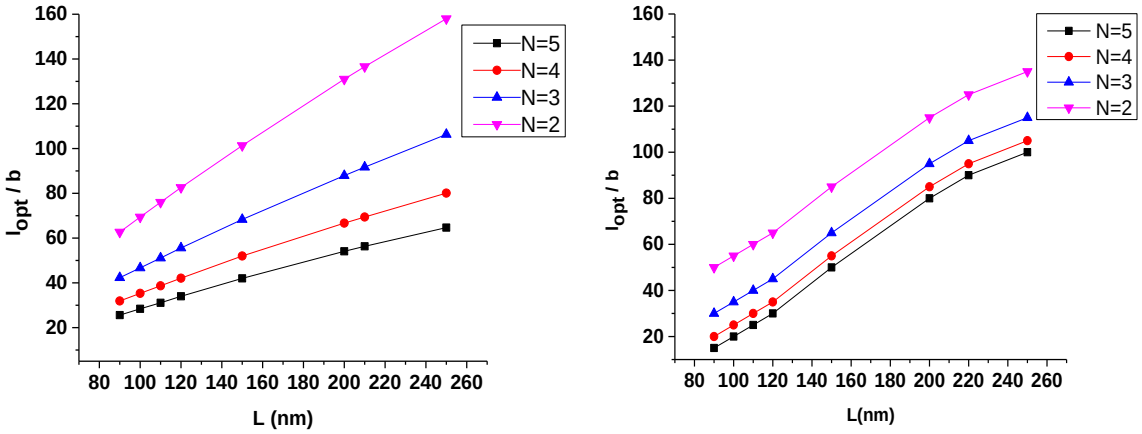

Figure 3.10: The number of the condensed monomers as a function of chain length. A system of 2, 3, 4, and5(a) G3 and (b)G4 complexes with an oppositely charged flexible LPE of persistence length of 50nm and monomers spacer of 0.7nm.100nm of Debye screening length.

3.6 Effect of Chain Stiffness (Persistence length) on PAMAM Dendrimer – LPE Complex Conformation:

The condensed monomers of the flexible LPE chain on the two dendrimer of Gx and the total charge of the complex are studied at different degrees of the chain rigidity; LPE chain length corresponds to total length of $440\,bp$. And because of this, the overcharging phenomenon of dendrimer will not occur. The LPE chain rigidity is measured in terms of persistence length which varied from 3nm to 50 nm, and considering the effect of Bjerrm length which is represented by values $l_B = 10b$ which represents the complex in the water solution, and Debye length = 16nm.

Figure 3.11 (a) shows the number of the condensed monomers of LPE on dendrimer and it shows that when l_p increases, the number of condensed monomers linearly decreases, and when the dendrimer size increase, the condensed monomers increases. This is due to the increase of rigidity of the LPE so it will affect the bending of LPE around the dendrimer.

Figure 3.11 (b) shows the total charge of the complex as a function of persistence length. The total charge of complex doesn't change significantly because of the electrical attractive free energy of PAMAM (G2, G4, G6, and G8) where $l_B = 10b$. Where the total charge slightly increases when the generation of dendrimer increases. It is expected for larger contour length of LPE chain (i.e., $L >> l_{iso}$), that the charge inversion phenomenon of the dendrimer will occur especially at $l_B = 10$b and gains its importance which means that the potential ability of LPE chain – dendrimer binding ability to cell membrane becomes more troublesome since the cell membrane is negatively charged.

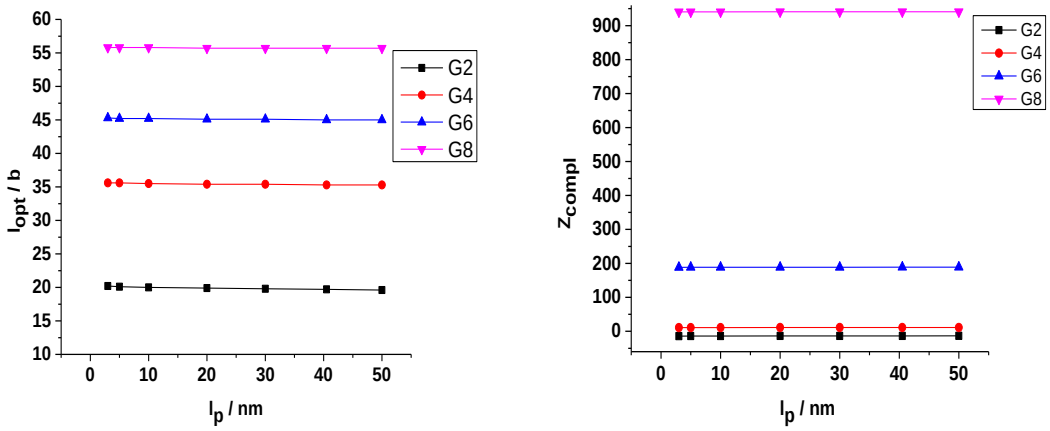

(a) **(b)**

Figure 3.11: The effect of persistence length lp on (a) the number of the condensed monomers of LPE on dendrimer of Gx and (b) the effective charge of the LPE chain – dendrimer complex, for a system of two dendrimer of Gx and an appositively charged flexible LPE of length $L = 150nm$ with bond spacer equals to 0.67nm, at 1:1 salt concentration corresponds to 16 nm of Debye length. The dendrimer was considered to be penetrable sphere of radius $R = 4nm$.

3.7 The Effect of the pH Value of the LPE Chain on the Linker Formed between 2G6, 2G4 – LPE Chain Complexes:

At high pH, the dendrimer is uncharged and the formation of any DNA-dendrimer complex is not formed and all amino groups of PAMAM dendrimers are deprotonated. At neutral pH, the dendrimer is positively charged due to the protonation of all the primary amines and hydrogen bonding between uncharged tertiary amines. The strong electrostatics interaction helps the DNA strand collapse onto the dendrimer. At low pH, the complex is formed too much of DNA conformation, due to repulsions force between primary and tertiary positively charged amines in the interior and surface of the dendrimer (see Table 3.5). The composition formed between flexible LPE of 680 nm length chain (541 bp) and persistence length $lp = 3\ nm$ with charge spacing of

the chain is $b = 0.17nm$, and two PAMAM dendrimers of G6 and G4 have been studied, by applying the penetrable sphere model, in aqueous solutions containing 10mM 1:1salt which corresponds to $6nm$ of Debye screening length and $0.71nm$ of Bjerrum length.

We present in Figure 3.12 the effect of pH value on the linker formed between 2G6, 2G4– LPE complexes and the optimal wrapping length of LPE chain around PAMAM dendrimer of G6, G4.By using a fix total charge , degrees are 405e and 126e and radius 3.55nm and 4nm for each pH value 5.5 and 8.5 respectively, and different values of total charge and radius according to all generation in neutral pH $(\mathrm{pH} = 7)$ .We can accord the increase of optimal wrapping length around dendrimer in acidic condition, and a small wrapping length in complete for high pH value. But in the case of G4 larger values G6 in more acidic conditions, we have the largest wrapping length of LPE chain around dendrimer. As a result the linker formed between complexes is small.

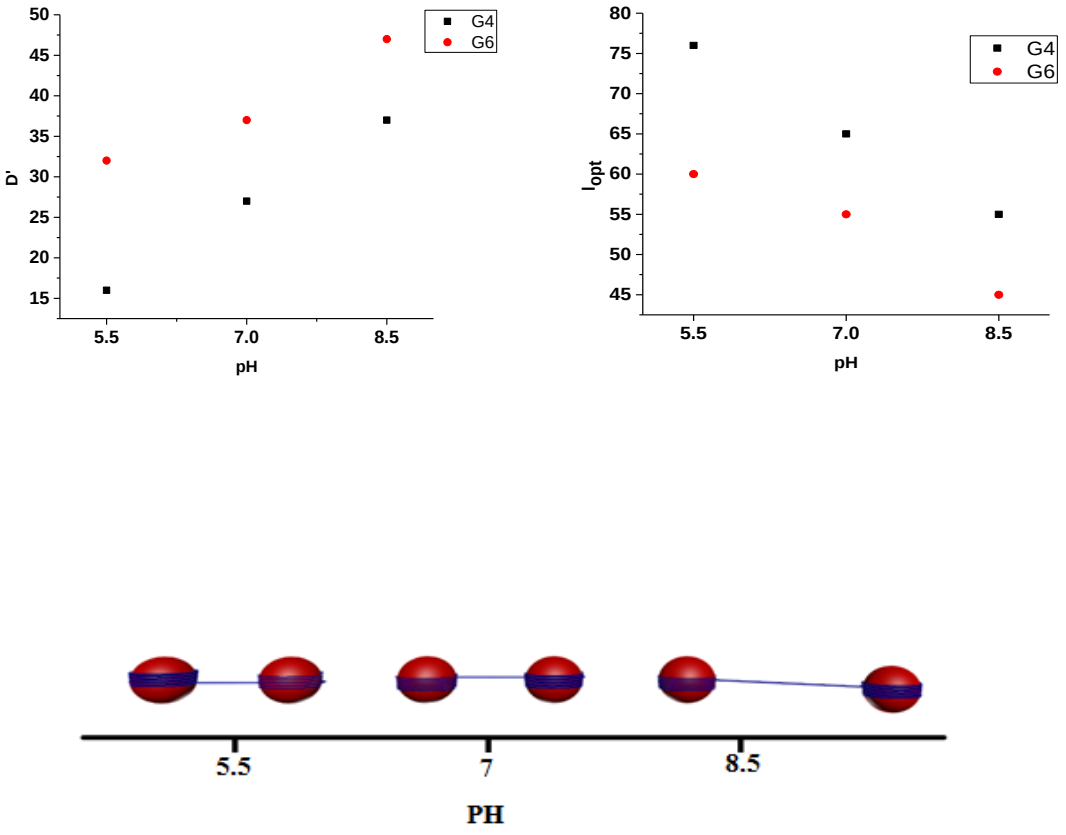

(c)

Figure 3.12: (a) linker formed between 2G6, 2G4- DNA complexation as a function of pH value, (b) l_{opt} formed between 2G6, 2G4- DNA comlexation as a function of pH value, (c) linker formed between 2G6 – DNA complexation as a function of pH value. The LPE chain molecules of 541 bp (184 nm), the dendrimers are considered as penetrable spheres with radius R.

	G4				G6			
pH	total charge	l_{opt}	Linker(D')	Radius(nm)	total charge	l_{opt}	Linker (D')	Radius(nm)
5.5	126	76	16	4.66	405	60	32	3.55
7	64	65	27	4.5	256	55	37	2.6
8.5	16	55	37	4	160	45	47	3.04

Table 3.5: Analytical model results for the interaction between 2 G6 and 2G4 dendrimers and LPE chain (541 bp), length $L = 184\,nm$ the dendrimers considered as a penetrable sphere with radius R.

CHAPTER FOUR

Conclusion and Future Work

Chapter 4: Conclusion and Future Work

4.1Conclusion and Future Work

We have studied the structure of the complexes formed by multi-dendrimer and an oppositely charge, LPE by using the penetrable sphere model. The increase of the LPE in complexes leads to the linker appearance between dendrimers surprisingly. The linker size depends on the LPE length non-monotonously.

The wrapping length of the LPE chain of length 680nm around dendrimer of different generations G1, G2, G3, G4, G6, and G8 in the aggregate doesn't change significantly irrespective how much dendrimer contracts due to the complexation with the oppositely charged LPE chain. As a consequence, the net charge of the complexes doesn't change which is negative for all aggregates of different generations with the exception of G4. In other words, the aggregate formed by dendrimer G4 – LPE complexes bears a slightly positive and fixed total charge whatever the dendrimer contracts.

The effect between a multiple PMAMAM dendrimer- LPE chain complexes showed that optimal wrapping length increases by decreasing the linker. The total length of LPE chain is divided into two parts, the linker and the optimal wrapping length, so the optimal wrapping length increases with increasing LPE length and linker.

We concluded that the wrapping length of the LPE chain depends on dendrimer generations. For lower generations G2 –G4, the optimal wrapping length of LPE around dendrimer increases significantly, and more of the LPE chain charges get neutralized. This could mean that the size of the aggregate of the complexes will increase. Whereas for higher generation G6 – G8, there is no significant increase in the optimal wrapping length of LPE chain around dendrimer. This means that the aggregate formed by the complexation between LPE and dendrimers of higher generations is insensitive to ionic strength. In other words, the aggregate formed from the complexation between LPE

chain with dendrimers of higher generation seems to be more neutralized than those formed of lower generations. This result is in agreement with the experimental study carried by **[Carnerup et al., 2011]**

In conclusion, the model presented for complexation of LPE with a penetrable sphere is suitable to represent the complexation of DNA with dendrimer since a lot of our results are in agreement with a series of computer simulations carried by **[Lyulin et al., 2008]**

We can accord the decrease of optimal wrapping length around dendrimer,in all cases as the persistence length of the chain is increased. The effect of chain stiffness is different from dendrimer according to the difference in radius, charge value and generation of dendrimer.

Despite of this, minor modifications could be inserted on the developed model. For a strongly charged spherical complex of charge$Z(l)e$, also for highly charged LPE chain, the repulsive electrostatic between the charged monomers should be added to the total free energy. The present analytical study has a great practical significance and promises to be an exciting area for further research in gene therapy. We expect that more results could be obtained by this new developed model.

Finally, Dendrimer hold a promising future in various pharmaceutical application and diagnostic field in the coming years, as they possess unique properties, such as higher degree of branching, multivalency, globular architecture and well-defined molecular weight; thereby offering new scaffold for drug delivery. Also as newer application of dendrimer will stand out and the future should evidence an increasing number of commercialized dendrimer based for drug delivery systems.

Appendix A: Schiessel Model

In this appendix the researcher presents the model developed by Schiessel and co-workers (Schiessel et al., 2001) which describes the complexation between hard sphere of radius R, charge Ze and semiflexible rod of radius a = 1nm and contour length L, where L>>R. They restricted their study to the highly charged chain as the charge of PE chain per unit length is -e / b, where b is the distance between the charges on the chain equals to 0.17nm which is much smaller than Bjerrum length l_B. According to the experimental conditions, the salt solution is characterized by Bjerrum length $l_B = e^2/\varepsilon k_B T$($\varepsilon$: dielectric constant of the medium; at room temperature gives l_B = 0.71nm) and Debye screening length is $\kappa^{-1} = (8c_s\pi l_B)^{-1/2}$($c_s$: Concentration of salt; κ^{-1} value is large compared to the radius of the sphere).

The total free energy for a system consists of a PE chain and a single hard sphere was proposed by them as follows:

$$F_l = F_{compl}\,(l) + F_{chain}\,(L-l) + F_{compl-chain}\,(l) + F_{elastic}\,(l) \qquad \text{(A.1)}$$

where L is the contour length of the DNA, and l is the length of the part of the chain wrapped around the hard sphere (Dendrimer).

The first term is the electrostatic charging free energy of a spherical complex of charge $Z(l)e$.

$$F_{compl}(l) \cong \begin{cases} \frac{e^2 Z^2\,(l)}{2\varepsilon R} & for \;\; |Z(l)| < Z_{max} \\ |Z(l)| k_B T\, \omega\big(Z(l)\big) & for \;\; |Z(l)| \gg Z_{max} \end{cases} \qquad \text{(A.2)}$$

Here, k_B is a Boltzmann constant, Z_{max} is the effective charge of the sphere and of order $\Omega R/l_B$ (Alexander et al., 1984), $Z(l) = Z - l/b$ and ε is the dielectric constant of water.

where $\omega\left(Z(l)\right)$ is the entropic cost to confine counterions close to highly charged sphere .

$$\omega\left(Z(l)\right) = 2\ln\left(\frac{|z(l)|\, l_B \kappa^{-1}}{R^2}\right) \quad \text{(A.3)}$$

The second term of the total entropic electrostatic free energy of the remaining chain $(L-l)$ has been given by

$$F_{chain}(L-l) \cong \frac{k_B T}{b}\, \Omega(a)(L-l) \quad \text{(A.4)}$$

where $\Omega(a)$ is the entropic cost to 'confine' counterions close to the chain and given by

$$\Omega(a) = 2\ln\left(\frac{4\xi\kappa^{-1}}{a}\right) \quad \text{(A.5)}$$

And a Manning parameter, describing counterions condensation on the chain

$$\xi = \frac{l_B}{b} \quad \text{(A.6)}$$

The third term is the electrostatic free energy of the interaction between the complex and the remainder of the chain (unwrapped part), given by

$$F_{cmpl-chain}(l) \cong Z(l) k_B T \ln(\kappa R) \quad \text{(A.7)}$$

where $Z(l)$ is the effective charge of the complex, and is the inverse of Debye screening length.

The final term is the elastic (bending) free energy required to bend l of the chain of Radius R around the hard sphere.

$$F_{elastic}\,(l) \cong \frac{k_B T l_p}{R^2}\, l \quad \text{(A.8)}$$

lp is the persistence length of the chain as defined above and R the radius of the PE chain.

Schiessel extended his model for a system consisting of one PE chain and N number of hard spheres.He expressed the free energy for the aggregate by:

$$F(N,l) = NF(l) + F_{int}(N,l) \quad \text{(A.9)}$$

where $F(l)$ is the total free energy of the PE chain-sphere complex as expressed in Eq.(A.1) $F_{int}\ which$ is the electrostatic repulsion between all complexes on the beads on a string configuration, and is obtained from summing over the electrostatic repulsion between all complexes within one molecule. The repulsive electrostatic interaction free energy can be expressed as:

$$F_{int}(N,l) \cong \Lambda k_B T \frac{N l_B Z^2(l)}{D(N,l)} \quad \text{(A.10)}$$

$D(N,l)$ is the center-to-center distance between two neighboring spheres and equal $(L - Nl + 2NR) / N$, Λ is logarithmic factor of the order $\ln(\kappa^{-1}/D)$

Eq. (A.10) is worth noting that this term will be small if the complex charge is close to neutral when $Z(l = l_{iso}) = 0$.

The total free energy for PE – dendrimer aggregate in Eq. (A.9) can be expressed as

$$\frac{F_{int}(N,l)}{k_B T} \cong \frac{l_B N}{2R} Z^2(l) + A\ \frac{l}{b} N - N\omega Z + \frac{\Lambda N^2 l_B Z^2(l)}{D(N,l)} + \ln(\kappa R) NZ \quad \text{(A.11)}$$

With

$$A = \frac{l_p b}{R^2} - \ln(\kappa R) - \Omega \quad \text{(A.12)}$$

Appendix B: Electrostatic Interaction between two Penetrable Spheres

If a uniformly charged sphere immersed in a liquid containing N ionic species with valence z_i and bulk concentration $n_i (i = 1, 2, \dots, N)$, the electric potential $\varphi(r)$ at position r, is measured relative to the bulk solution phase, given by Poisson equation (Ohshima, 2010).

$$\Delta\varphi(r) = -\frac{\rho_{el}(r)}{\varepsilon_r \varepsilon_0} = -\frac{\rho_{el}(r)}{\varepsilon} \quad \text{(B.1)}$$

Where Δ is the Laplacian, $\varepsilon = \varepsilon_r \varepsilon_0$ which is the relative permittivity of the electrolyte solution, and ε_0 is the permittivity of the vacuum. The distribution of the electrolyte ions $n_i(r)$ obeys Boltzmann law, given by

$$n_i(r) = n_i^{\infty} e^{-\frac{z_i e \varphi(r)}{k_B T}} \quad \text{(B.2)}$$

where n_i^{∞} is the concentration of the total number of ions in electrolyte solution, $n_i(r)$ is the concentration of the ith ion at position r, e is the elementary electric charge, k_B is the Boltzmann constant, and T is the absolute temperature. The charge density $\rho_{el}(r)$ at position r is given by

$$\rho_{el}(r) = \sum_{i=1}^{N} z_i e n_i(r) = \sum_{i=1}^{N} z_i e n_i^{\infty} e^{-\frac{z_i e \varphi(r)}{k_B T}} \quad \text{(B.3)}$$

Substituting Eq. (B.3) into Eq. (B.1) gives:

$$\Delta\varphi(r) = -\frac{1}{\varepsilon} \sum_{i=1}^{N} z_i e n_i^{\infty} e^{-\frac{z_i e \varphi(r)}{k_B T}} \quad \text{(B.4)}$$

This is the Poisson-Boltzmann equation for the potential distribution $\varphi(r)$. If the potential is low, then the term is

$$\left|\frac{z_i e\varphi}{k_B T}\right| \ll 1$$

By the expansion of the exponential terms in the summation in Eq. (B.3) gives:

$$\rho_{el}(r) = \sum_{i=1}^{N} z_i e n_i^{\infty} \left[1 - \left(\frac{z_i e\varphi(r)}{k_B T}\right) + \frac{1}{2!}\left(\frac{z_i e\varphi(r)}{k_B T}\right)^2 - \cdots\right] \quad \text{(B.5)}$$

The first term in the summation vanishes because of the condition of electroneutrality, i.e.,

$$\rho_{el}(r) = \sum_{i=1}^{N} z_i e n_i^{\infty} = 0 \quad \text{(B.6)}$$

By taking only the linear term in Eq. (B.5), then Eq. (B.4) becomes

$$\Delta\varphi(r) = \frac{1}{\varepsilon k_B T} \sum_{i=1}^{N} z_i^2 \, e^2 n_i^{\infty} \varphi(r) \quad \text{(B.7)}$$

Also Eq. (B.7) can be written in the linearized form

$$\Delta\varphi(r) = \begin{cases} \kappa^2\varphi(r), outside\ the\ sphere \\ \kappa^2\varphi(r) - \frac{\rho}{\varepsilon}, inside\ the\ sphere \end{cases} \quad \text{(B.8)}$$

With

$$\kappa = \left(\frac{1}{\varepsilon k_B T}\sum_{i=1}^{N} z_i^2 e^2 n_i^{\infty}\right)^{1/2} \qquad \text{(B.9)}$$

Eq. (B.8) is the linearized Poisson-Boltzmann equation and κ is the Debye-Hückel parameter. Also, Eq. (B.8) is called the Debye-Hückel equation. The reciprocal of κ is called the Debye length.

The electrostatic free energy of ion-penetrable sphere and the electrostatic interaction free energy between two ion-penetrable spheres have been given by the linearized Poison-Boltzmann equation by Ohshima where he considered two identical interacting charged ion-penetrable spherical particles, (i.e., two charged porous spheres) as shown in Figure B.1 of equal fixed charge density ρ and equal radii R, separated by a distance D between their centers (Ohshima, 1993).

He considered the unperturbed potential φ_1 produced by sphere 1, since the potential of a single isolated sphere is spherically symmytric, the linearized Poison-Boltzmann equations for φ_1 depend only on r_1 and reduce to

$$\frac{d^2\varphi_1}{dr_1^2} + \frac{2}{r_1}\frac{d\varphi_1}{dr_1} = \kappa^2\varphi_1, r_1 > R \qquad \text{(B.10)}$$

$$\frac{d^2\varphi_1}{dr_1^2} + \frac{2}{r_1}\frac{d\varphi_1}{dr_1} = \kappa^2\varphi_1 - \frac{\rho}{\varepsilon}, 0 \leq r_1 < R \qquad \text{(B.11)}$$

These equations can be solved by using the variables substitution

$$\varphi_1(r_1) = \frac{u_1(r_1)}{r_1} \tag{B.12}$$

The homogenous differential equation, i.e., Eq. (B.10), appears as the following

$$\frac{d^2u_1}{dr_1^2} = \kappa^2 u_1 \, , r_1 > R \tag{B.13}$$

Thus Eq. (B.10) has the general solution of the form

$$\varphi_1(r_1) = E\frac{e^{\kappa r_1}}{r_1} + F\frac{e^{-\kappa r_1}}{r_1} \tag{B.14}$$

Also the non-homogenous differential equation in Eq. (B.11) can be expressed as

$$\frac{d^2u_1}{dr_1^2} - \kappa^2 u_1 = -\frac{\rho}{\varepsilon} r_1 \, , r_1 > R \tag{B.15}$$

The general solution of Eq. (B.11) has the form

$$\varphi_1(r_1) = G\frac{e^{\kappa r_1}}{r_1} + H\,\frac{e^{-\kappa r_1}}{r_1} + \frac{\rho}{\varepsilon k^2} \tag{B.16}$$

where$E$, F, G, and H are undetermined constants, the boundary conditions are

$$\varphi_1(r_1 \to \infty) = 0, \varphi_1(R+) = \varphi_1(R-), and \;\; \left.\frac{d\varphi_1}{dr_1}\right|_{r1=R+} = \left.\frac{d\varphi_1}{dr_1}\right|_{r1=R-} \tag{B.17}$$

Then, Eqs. (B.10) and (B.11) are solved easily and subject to the above boundary conditions, give:

$$\varphi_{sphere\,1} = \frac{\rho}{\varepsilon\kappa^2}\, R\, \left[\cosh(\kappa R) - \frac{\sinh(\kappa R)}{\kappa R}\right] \frac{e^{-\kappa r_1}}{r_1} \, , r_1 > R \tag{B.18}$$

The unperturbed potential produced by sphere 2, obtained by replacing r_1 with r_2, here r_2 is the radial coordinate measured from the center of sphere 2 (see Figure B.1), which is related to r_1 by the relation

$$r_2 = (D^2 + r_1^2 - 2Dr_1 \cos\theta\ )^{1/2} \qquad \text{(B.19)}$$

Gives

$$\varphi_{sphere\,2} = \frac{\rho}{\varepsilon\kappa^2}\ R\ \left[\cosh(\kappa R) - \frac{\sinh(\kappa R)}{\kappa R}\right] \frac{e^{-\kappa r_2}}{r_2}\ , r_2\ > R \qquad \text{(B.20)}$$

Then Ohshima found the electrostatic interaction free energy between ion-penetrable spheres on the bases of Verwey and Overbeek method (Verwey and Overbeek, 1948). This method is based on a charging process in which all the particle-fixed charges are increased at the same rate. The free energy for one sphere was obtained by the charging integral

$$F_{sphere}\ = \frac{1}{2}\int_v \rho\varphi_{sphere}\, dv \qquad \text{(B.21)}$$

The integration is carried out over the volume v , where ρv is the final charge on each sphere i.e.,$Q = Ze = \rho v$, which equals to $4\pi\rho\ /3R^3$. He got:

$$F_{sphere}\,(Z) = \frac{3Z^2e^2}{8\pi\varepsilon(\kappa R)^2}\ \left[\cosh(\kappa R) - \frac{\sinh(\kappa R)}{\kappa R}\right] \frac{e^{-\kappa R}}{R} \qquad \text{(B.22)}$$

The electrostatic interaction free energy can be expressed as the free energy of a system of two spheres at separation D between their centers minus that at infinite separation.

$$F_{int} = F(D) - F(\infty) \qquad \text{(B.23)}$$

Where, $F(D)$ is the free energy of two spheres at separation D between their centers, $F(\infty)$ is the free energy of two spheres at an infinite separation. To find the electrostatic interaction energy between two spheres, he needs only to obtain the potential

distribution produced within sphere1 by sphere 2. Thus Ohshima wrote the charging integral in the form

$$F_{int} = \frac{1}{2} \int_{\nu} \rho \varphi_{sphere2} \, d\nu_1 \tag{B.24}$$

Using the spherical coordinates, the element volume of sphere 1 was given by

$$d\nu_1 = 2\pi r_1^2 \sin\theta \, d\theta dr_1 \tag{B.25}$$

substituting Eq (B.20) into Eq. (B.24) and using Eq. (B.25). Then, the interaction free energy between two ion-penetrable spheres has been given by:

$$F_{int} = \frac{1}{2} \frac{\rho^2}{\varepsilon\kappa^2} \, R \left[\cosh(\kappa R) - \frac{\sinh(\kappa R)}{\kappa R}\right] \int_{\nu 1} \frac{e^{-\kappa r_2}}{r_2} \, d\nu_1 \tag{B.26}$$

The integral in the RHS of the above equation can be evaluated as follows:

$$\int_{\nu} \frac{e^{-\kappa r_2}}{r_2} \, d\nu_1 = \frac{e^{-\kappa\left(D^2 + r_1^2 - 2Dr_1\cos\theta\right)^{\frac{1}{2}}}}{\int_0^R \int_0^{\pi} \left(D^2 + r_1^2 - 2Dr_1\cos\theta\right)^{\frac{1}{2}}} \times r_1^2 \sin\theta \, dr_1 d\theta \tag{B.27}$$

$$= \frac{4\pi}{\kappa^2} R \left[\cosh(\kappa R) - \frac{\sinh(\kappa R)}{\kappa R}\right] \frac{e^{-\kappa D}}{D}$$

Then, the interaction free energy between two ion-penetrable spheres can be expressed as:

$$F_{int} = \frac{2\pi\rho^2}{\varepsilon\kappa^4} \, R^2 \left[\cosh(\kappa R) - \frac{\sinh(\kappa R)}{\kappa R}\right]^2 \frac{e^{-\kappa D}}{D} \tag{B.28}$$

Bibliography

A. Akinchina and P. Linse, (2002), Monte Carlo Simulations of Polyion−Macroion Complexes. 1. Equal Absolute Polyion and Macroion Charges Macromolecules, 35, 5183-5193

A.V. Dobrynin, J. (2001), Molecular Dynamics Simulations of Polyelectrolyte Adsorption.Chem. Phys., 114, 8145.

Ainalem M.L., Nylander T., DNA (2014), condensation using cationic dendrimer-morphology and superamolecular structure of formed aggregates, soft matter, 7, 4577.

Ainalem, M. L., Carnerup, A. M., Janiak, J., Alfredsson, V., Nylander, T., (2009) Condensing DNA with poly (amido amine) dendrimers of different generations: means of controlling aggregate morphology, Soft Matter, 5, 2310–2320.

Berg J., Tymoczko J. and Stryer L. (2002) Biochemistry. W. H. Freeman and Company.

Bielinska, A. U., Chen, C., Johnson, J., Baker, J. R., (1999), DNA Complexing with Poly (amidoamine) Dendrimers, Implications for Transfection, Bioconjugate Chem., 10, 843–850

Boroudjerdi, H., Naji, A., Netz., R. R., (2011), Salt Modulated Structure of Polyelectrolyte- Macroion Complex Fibers, cond. mat. Soft, 1-17.

Carnerup, A. M., Ainalem, M. L., Viveka, A., Nylender, T., (2011), Condensation of DNA using poly (amido amine) dendrimers: effect of salt concentration on aggregate morphology, Soft Matter, 7, 760–768.

Chai Ai-Hua, Ran Shi-Yong, Zhang Dong, (2013) Processes of DNA condensation induced by multivalent cations : Approximate annealing experiments and molecular dynamics simulations. Chin. Phys. B, 22(9): 098701.

Cheng, Y., Zhenhua, X., Minglu, M., Tongwen, X., (2008), Dendrimers as drug carriers: applications in different routes of drug administration, J. Pharm. Sci., 97, 123–143.

Cormac Sheridan, (2011) Gene therapy finds its niche, Nature Biotechnology 29, 121–128

El-Sayed., (2001), some interesting properties of metals confined in time and nanometer space of different shapes, Acc Chem Res. 34(4):257-64.

Fant, K., Esbjorner, E. K., Jenkins, A., Grossel, M. C., Lincoln, P., Norden, B., (2010), Effects of PEGylation and acetylation of PAMAM dendrimers on DNA Binding, cytotoxicity and in vitro transfection efficiency, Mol. Pharm., 7, 1743–1746.

Fant, K., Esbjorner, E. K., Lincoln, P., Norden, B., (2008), DNA Condensation by PAMAM Dendrimers: Self-Assembly Characteristics and Effect on Transcription Biochemistry, 47, 1732-1740.

Hagerman P., J., (1988), Flexibility of DNA, Annual Review of Biophysics and Biophysical Chemistry, Vol. 17: 265-286.

Halford, B., (2005), Dendrimers branch out, Chem. Eng. News, 83, 30–36.

Itaka, K., Kataoka, K., (2009), recent development of nonviral gene delivery systems with viruslike structures and mechanisms, Eur J. Pharm Biopharm., 71, 475–483.

Jackson, J. L., Chanzy, H. D., Booy, F. P., Drake, B. J., Tomalia, D. A., Bauer, B. J., Amis, E. J., (1998), Visualization of dendrimer molecules by transmission electron (TEM): staining methods and Cryo-TEM of vitrified solutions, Macromolecules, 31, 6259–6265.

Kataoka K, Harashima H., (2001), Gene delivery systems: viral vs non-viral vectors. Adv Drug Deliv Rev., 52. 151.

Kukowska-Latallo, J. F., Candido, K. A., Cao, Z., Nigavekar, S. S., Majoros, I. J., Thomas, T. P.,Balogh, L. P., Khan, M. K., Baker, J. R. (2005), Improves Therapeutic Response in Animal Model of Human Epithelial, J. Synthesis, 65, 5317–5324.

Kunze, K. K., Netz, R. R., (2002), Complexes of semiflexible polyelectrolytes and charged spheres as models for salt-modulated nucleosomal structures, physical review E 66, 011918, 1-28.

Larin, S. V., Lyulin, S. V., Darinskii, A. A., (2009), Charge Inversion of Dendrimers in Complexes with Linear Polyelectrolytes in the Solutions with Low pH Polymer Science, Ser ., 51, 459–468.

Larin, S.V., Darinskii, A. A., Lyulin, A. V., Lyulin, S. V., (2010), Linker Formation in an Overcharged Complex of Two Dendrimers and Linear Polyelectrolyte, J. Phys. Chem., 114, 2910-2919.

Larin, S.V., Darinskii, A. A., Lyulin, A. V., Lyulin, S. V., (2010), Linker Formation in an Overcharged Complex of Two Dendrimers and Linear Polyelectrolyte, J. Phys. Chem., 114, 2910-2919.

Lee, C. C., Mackay, J. A., Frechet, J. M. J., Szoka, F. C., (2005), Designing dendrimers for biological applications, Nat. Biotechnol., 23, 1517–1526.

Lee, H., Larson, R. G., (2009), Multiscale Modeling of Dendrimers and Their Interactions with Bilayers and Polyelectrolytes, Molecules, 14, 423-438.

Leonard C. Gosule, John A. Schellman, (1978), DNA condensation with polyamines, Journal of Molecular Biology Volume 121, Pages 311–326.

Liu Y., Wang W., Hu L., (2012), Dependence of DNA condensation on the correlation distance between condensed counter ions, J Biol Phys. 38(4): 589–596.

Lyulin, S. V., Darinskii, A.A., Lyulin, A. V., (2005), Computer Simulation of Complexes of Dendrimers with Linear Polyelectrolytes, Macromolecules, 38, 3990-3998.

Lyulin, S.V., Vattulainen, L., Gurtovenko, A. A., (2008), Complexes Comprised of Charged Dendrimers, Linear Polyelectrolytes, and Counterions: Insight through Coarse-Grained Molecular Dynamics Simulations. Macromolecules, 41, 4961-4968.

Manning Q., (1978), Counterion condensation theory, Revs. Biophys. 11, 179-24.

Marta Sowinskaa and Zofia, rbanczyk-Lipkowska, Advances in the chemistry of dendrimers (2014) New J. Chem., 2014, 38, 2168-2203,

Mateescu, E. M., Jeppesen, C., Pincus, P., (1999), Overcharging of a spherical macroion by an oppositely charged polyelectrolyte, Europhys. Lett., 46, 493.

Netz, R. R., Joanny, J. F., (1999), Complexation between a Semiflexible Polyelectrolyte and an Oppositely Charged Sphere, Macromolecules, 32, 9026.

Newkome, G. R., Yao, Z. Q., Baker, G. R., Gupta, V. K. (1985), Micelles Part 1. Cascade molecules: a new approach to micelles, J. Org. Chem., 50, 155–158.

Nguyen, T. T., Shklovskii, B. I., (2001), Overcharging of a macroion by an oppositely charged polyelectrolyte, Physica, A 293, 324–338.

Nomani, A., Haririan, I., Azizi, E., Foladdel, S., Dinarvand, R., Omidi, Y. and Gazori, T. (2010), Physicochemical Properties And Cell Culture Activity Of Self-Assembled Antisense Poly(Amidoamine) Dendrimer Nanoparticles: The Effect Of Dendrimer Generation And Charge Ratio, International Journal of Nanomedicine, 5, 1-11.

Örberg, M. L., Schillen, K., Nylander, T., (2007), Dynamic Light Scattering and Fluorescence Study of the Interaction between Double-Stranded DNA and Poly(amido amine) Dendrimers Biomacromolecules, 8, 1557.

Park, S. Y, Bruinsma, R. F., Gelbart, W. M., (1999), Spontaneous overcharging of macro-ion complexes, Europhys. Lett. 46,454.

Prabal K. Maiti, Tahir Cü ag, Shiang-Tai Lin, and William A. Goddard, (2004).

Prajapati, R. N., Tekade, R. K., Gupta, U., Gajbhiye, V., Jain, N. K., (2009), Dendimer-Mediated Solubilization, Formulation Development and in Vitro- in Vivo Assessment of Piroxicam, Synthesis, 6, 940–950.

Qamhieh K., Abukhaleel A., (2011). Analytical model study of complexation of dendrimer as an ion penetrable sphere with DNA, J. of Colloids and Surface, 442 191–198.

Qamhieh, K., Nylander T., Black, C, F, Attard, G, S., Dias, R, S., Ainalem, M. L., (2014), Complexes formed between DNA and poly(amido amine) dendrimer of different generation modeling DNA wrapping and penetration, the Owner Societies, 16, 13112-13122 .

Qamhieh, K., Nylander, T., Ainalem, M. L., (2009), Analytical Model Study of Dendrimer/DNA Complexes, Biomacromolecules, 10, 1720-1726.

Rolf Dootz, an Adriana Cristina Tomab, (2008), PAMAM6 dendrimers and DNA: pH dependent "beads-on-astring" behavior revealed by small angle X-ray scattering, Bunsenstrasse 10, 37073

Schiessel, H., (2003), the physics of chromatin, J. Phys.: Condens. Matter, 15, R699-R774.

Schiessel, H., Bruinsma, R. F., Gelbart, W. M., (2001), Electrostatic complexation of spheres and chains under elastic stress, J. of chemical physics, 115, 7245.

Svenson, S., Tomalia, D. A., (2005), Dendrimers in biomedical applications-reflections on the field, Adv. Drug Deliv. Rev., 57, 2106–2129.

The DNA,the DNA laboraterylimited,2015 , RUL :
http://www.thednall.com/images/what_img2

Tian, W., Ma, Y., (2010), Complexation of a Linear Polyelectrolyte with a Charged Dendrimer: Polyelectrolyte Stiffness Effects, Macromolecules, 43, 1575-1582.

Tomalia, D. A., (1993), Starburst/cascade dendrimers: fundamental building blocks for a new nanoscopic chemistry set. Aldrichim. Acta., 26, 91–101.

Tomalia, D. A., (2005), Birth of a new macromolecular architecture: dendrimers as quantized Building blocks for nanoscale synthetic polymer chemistry, Prog. Polym. Sci., 30, 294–324.

Tomalia, D. A., Naylor, A. M., Goddard III, W. A., (1990), Starburst Dendrimers: Molecular-Level Control of Size, Shape, Surface Chemistry, Topology, and Flexibility from Atoms to Macroscopic Matter, Angew. Chem. Int. Ed. Engl., 29, 138–175.

Wang, R., Zhou, L., Zhou., G., Li, G., Zhu, B., Gu, H., Jiang, X., Li., H., Wu, J., He, Guo L., , Zhu X.B., Yan, D., (2010), Synthesis and gene delivery of poly(amido amines) with different branched architecture. Biomacromolecules, 11, 489–495.

Watson, J., Crick, F., (1953), Molecular structure of nucleic acids; a structure for deoxyribose nucleic, Nature, 171(4356), 737-738.

Wen-de Tian, Yu-qiang Ma, (2012) .Insights into the endosomal escapes mechanism via investigation of dendrimer–membrane interactions, Journal Soft Matter Volume 8 Issue 23

الملخص

تكثيف الحمض النووي باستخدام دينديريمر موجب

بينت الدراسه كيفيه حدوث عمليه التجمع بين الدنديريمر والحمض النووي باستخدام كرة قابله للاختراق من قبل الايونات المحيطه **(ion-penetrable sphere)** وتمثلت هذه الدراسه باستخدام اثنين او اكثر من الدنديريمر من اجيال مختلفه **(G1)** و**(G2)** و**(G3)** و **(G4)** و **(G6)** و **(G8)** باستخدام نموذج نظري تم وضعه من قبل خوله قمحيه وعزام ابو خليل يصف التفاعل بين دنديريمر واحد ال **(LPE chain)** .

ولقد وجدت خلال هذه الدراسه ان درجه التفاف ال **(LPE chain)** حول الدنديريمر تزيد بزياده كل من الاجيال وعدد الدنديريمر وطول ال **(LPE chain)** وتركيز الملح في المحلول وتقل هذه الدرجه بزيادة صلابه ال **(LPE chain)**.

ولقد تم دراسة الطاقة الكهروستاتيكية **(electrostatic free energy)** لكل عنصر من هذا الترابط بهدف مقارنة النتائج مع نتائج التي حصل عليها عزام ابو خليل الترابط او التجمع الذي يحوي العديد من الدنديريمر مع **(LPE chain)** تبين ان درجه التفاف ال **(LPE chain)**) حول الدنديريمر تزداد بزياده شحنه الدنديريمر وتركيز الملح في المحلول وطول ال **(LPE chain)** تقل هذه الدرجه بزياده صلابه ال **(LPE chain)**.

اما بالنسبة **(Linker)** الذي يتكون بين الدنديريمر يقل بزيادة درجة التفاف **(LPE chain)** حول الدنديريمر ويزداد بزيادة **(pH)** في المحلول.